Transcriptome-wide identification and characterization of microRNAs in diverse phases of wood formation in *Populus trichocarpa*

Ruiqi Wang
Northeast Forestry University https://orcid.org/0000-0002-9403-7693
Mengxuan Ren
Northeast Forestry University
Shuanghui Tian
Northeast Forestry University
Cong Liu
Northeast Forestry University
He Cheng
Northeast Forestry University
Yingying Liu
Northeast Forestry University
Huaxin Zhang
Chinese Academy of Forestry
Saqib Muhammad
University of Agriculture Faisalabad
Hairong Wei
Michigan Technological University
Zhigang Wei (zhigangwei1973@163.com)
Chinese Academy of Forestry

Research article

Keywords: miRNA, target gene, primary stems, transition stems, secondary stems, Populus trichocarpa.

Posted Date: November 16th, 2020

DOI: https://doi.org/10.21203/rs.3.rs-108245/v1

Version of Record: A version of this preprint was published at G3 Genes|Genomes|Genetics on June 4th, 2021. See the published version at https://doi.org/10.1093/g3journal/jkab195.

Abstract

Background: MicroRNAs (miRNAs) are small, non-coding RNAs that have important regulatory functions in plant growth and development. However, the miRNAs that are involved in different developmental stages of tree stems have not been systemically characterized. In this study, we applied miRNA expression profiling method to the *Populus trichocarpa* trunks of the three distinct developmental stages defined as the primary stem (PS), transitional stem (TS), and secondary stem (SS) to investigate the miRNA species, their dynamic regulation and functions during the transitions of wood formation in different developmental stages at the genome-wide scale by Solexa sequencing.

Results: We obtained 892, 872, and 882 known miRNAs and 1,727, 1,723, and 1,597 novel miRNAs, from PS, TS, and SS, respectively. And identified 114, 306, and 152 differentially expressed miRNAs (DE-miRNAs) with 921, 2,639, and 2,042 candidate target genes (CTGs), which formed 158, 855, and 297 DE-miRNA-CTG pairs in PS vs TS, PS vs SS, and TS vs SS , respectively. Among these, 47, 439, and 71 DE-miRNA-CTG pairs showed a significant negative correlation, respectively. Finally, we identified 39, 9, and 92 miRNA-CTG pairs involved in PS, TS, and SS, respectively. These DE-miRNA-CTG pairs in poplar or whose counterparts in other plant species are known to be transcriptional factors or structural genes involved in cell division and differentiation, cell wall modification, secondary cell wall (SCW) biosynthesis, lignification, and programmed cell death processes of wood formation. Moreover, qRT–PCR analysis confirmed that the results of small RNA-seq were robust and reliable and most miRNA-CTG pairs exhibited an inverse correlation.

Conclusions: This is the first report on an integrated analysis of genome-wide mRNA and miRNA profiling of diverse phases of wood formation in poplar trunks. We showed that even though miRNAs involved in diverse developmental phases were not in a considerable number, their roles in the regulatory network that govern wood formation during different developmental stages cannot be negligible or underestimated. The information and data obtained in this paper significantly advanced our understanding of these miRNAs and their essential, dynamic and diversified roles as well as functions in diverse phases of wood formation in tree species.

1 Background

Wood represents the main source of terrestrial biomass production and is a major renewable resource for the timber, paper, and bioenergy industries [1]. Wood formation is a complexly continuous biological process involved in multiple molecular mechanisms to precisely control the collaborative expressions of many genes related to different processes of wood formation[1–3]. For example, a hierarchical transcriptional regulation network dominates secondary cell wall (SCW) formation, which mainly comprises the NAC and MYB transcription factor (TF) families and their regulated downstream structural genes related to SCW component biosynthesis and programmed cell death (PCD) [3, 4]. Alternative splicing has been reported to occur within some genes related to SCW formation, such as *CESA* and *CCoMT* [5]. Moreover, circRNAs were found to play essential roles in regulating genes involved in wood

formation via circRNA-miRNA-mRNA networks [6]. Until now, although extensive efforts have been made to unravel the molecular regulatory mechanisms of wood formation, a genome-wide profiling of both miRNAs and mRNAs across multiple developmental stages of wood formation may shed more lights on the underlying regulatory mechanisms.

MicroRNAs (miRNAs), a group of 20- to 24-nucleotide (nt) small non-coding RNAs, are sequence-specific regulators that function mainly via post-transcriptional mRNA cleavage or the inhibition of gene expression in eukaryotes [7]. More than 38,589 miRNAs have been identified (Release 22.1, October 2018; http://www.mirbase.org/). The available evidence indicates that miRNAs play influential roles in plant growth and development [7, 8]. For example, miR393 participates in primary growth by repressing *TIR1/AFBs*, auxin receptor F-box genes [9]. csn-miR319c regulates apical bud burst by suppressing *CsnTCP2* in tea [10]. miR528 promotes rice flowering by repressing *OsRFI2* under long-day conditions [11]. Presently, although some miRNAs, such as miR875 [12], ptr-miR397a [13], amg-miR166 [14], Pto-miR257 [15], Pto-MIR475b [16], and miRNA156 [17], have been identified to participate in different processes of wood formation [14, 18], no investigation has been reported on the dynamics of miRNAs and their biological functions involved in diverse phases of wood formation in tree species.

Presently, small RNA deep sequencing has emerged as a useful tool for plant miRNA rapid discovery, in which both the conserved and novel and lowly expressed miRNAs can be identified, and their abundances profiled simultaneously [19]. To date, hundreds of small RNAs have been successfully isolated from model plants and non-model plants using this method [19]. Moreover, because the expression levels of miRNAs display negative correlations with the expression levels of their target genes owing to transcript cleavage or translation repression [20, 21], the biological functions of miRNAs can be effectively identified by integrated analysis of the miRNA and mRNA expression profiles [21, 22]. For example, through integrated analysis of the miRNA and mRNA profiles, some miRNAs have been identified to regulate the rapid growth of developing culms in *moso bamboo* [22], five miRNAs were found to be involved in ethylene-regulated petal growth in *Rosa hybrida* [23], and miR156a, miR157a, and miR172a have been validated to play important roles in the tuberous root development of *Brassica rapa* [24].

The stems of less than one-year-old poplar trees mainly comprise three developmental stages that include most of the processes of wood formation [25, 26]. For example, the segments near the apical meristems, where cells mainly undergo division and expansion and synthesis of the primary cell wall, are the primary stems (PS) and represent the beginning phase of wood formation. By contrast, the segments in the basal portions, where cells undergo SCW biosynthesis, lignification, and PCD, are secondary stems (SS) and represent the late phase of wood formation. Additionally, segments in the middle of PS and SS, where cells synthesize SCW components in the inner part of the primary wall, are transition stems (TS) and represent the middle phase of wood formation. Thus, the different vertical segments of less than one-year-old poplar trees have been used to investigate the dynamics of gene expression and molecular regulatory mechanisms underlying diverse phases of wood formation [25–28]. In this paper, we concurrently generated the miRNA and mRNA expression profiles in the PS, TS, and SS of *Populus trichocarpa* using Solexa sequencing. This study was designed to collect data and gain insight into three

problems: (i) the dynamics of miRNAs associated with diverse phases of wood formation; (ii) the identification of the miRNA-mRNA model associated with diverse phases of wood formation; and (iii) the authentication of the biological functions of miRNAs related to diverse phases of wood formation. The sRNA-seq and RNA-seq data acquired constituted valuable genetic resources, and the results would be helpful for further studies of miRNAs involved in diverse processes of wood formation.

2 Results

Small RNAs in diverse developmental stages of *P. trichocarpa* stems

To identify the miRNAs involved in diverse phases of wood formation, we performed high-throughput sequencing of small RNA libraries generated from PS, TS, and SS, and obtained 15,374,878, 15,653,777, and 11,989,204 high-quality reads, respectively. Subsequently, the adapter sequences, poly A sequences, sequences < 18 nt, and other artifacts were removed, obtaining 14,705,980, 14,516,320, and 10,955,984 clean reads from PS, TS, and SS, respectively (Table S1). After the further removal of rRNAs, tRNAs, snRNAs, snoRNAs, repeat-associated small RNAs (sRNAs), and exon and intron sequences, we finally obtained 12,237,495, 11,639,629, and 9,336,272 sRNA reads in PS, TS, and SS, respectively (Table 1). Among these sRNAs, non-annotated sRNAs accounted for the greatest proportion of sRNAs, about 31.17%, 32.12%, and 23.18% of the total tag abundances in PS, TS, and SS, respectively (Table 1). These sRNAs were used to predict and identify novel miRNAs implicated in wood formation of poplar.

Table 1
Distribution of tags among different categories in PS, TS, and SS of P. trichocarpa

Sample	PS	%	TS	%	SS	%
Total	14705980	100.00%	14516320	100.00%	10955984	100.00%
rRNA	573687	3.90%	883279	6.08%	544309	4.97%
snRNA	14216	0.10%	16238	0.11%	9851	0.09%
snoRNA	33487	0.23%	26283	0.18%	10808	0.10%
tRNA	64517	0.44%	93329	0.64%	51681	0.47%
Exon sense	624595	4.25%	723074	4.98%	431574	3.94%
Exon antisense	309513	2.10%	269977	1.86%	140055	1.28%
Intron sense	584685	3.98%	584392	4.03%	276301	2.52%
Intron antisense	208812	1.42%	210260	1.45%	109456	1.00%
Repeat	54974	0.37%	69860	0.48%	45677	0.42%
miRNA	7653018	52.04%	6977646	48.07%	6796138	62.03%
non-annotated sRNA	4584477	31.17%	4661983	32.12%	2540134	23.18%

Most of the total sRNA reads of PS, TS, and SS ranged from 18 to 24 nt in lengths (Fig. 1), slightly different than the typical size range (20–24 nt) for Dicer-derived products [29], and the 21- and 24-nt sRNA accounted for most of the sRNAs and represented the plurality of sRNAs. The abundance of 21-nt sRNAs was significantly higher than that of sRNAs of any other lengths, and 24-nt sRNA represented the second highest abundant sRNA (Fig. 1). The abundance of 21-nt sRNA in SS accounted for 64.28% of all sRNAs and was significantly higher than the abundances of 54.56% and 49.9% of all sRNAs in PS and TS, respectively (Fig. S1). By contrast, the abundance of 24-nt sRNA accounted for 9.05% of all sRNAs in SS and was significantly lower than the abundances of 17.59% and 17.77% of all sRNAs in PS and TS, respectively (Fig. S1). These results suggest that differences exist in the sRNA lengths among PS, TS, and SS in poplar.

Known and novel miRNAs in the diverse developmental stages of *P. trichocarpa* stems

In this study, only the miRNAs whose precursors can form hairpin structures were considered. According to this criterion, we aligned all sRNAs identified from PS, TS, and SS with miRNA sequences present in miRBase22.1 of *P. trichocarpa.* Those sRNAs that could not be annotated to any known miRNAs were then used to identify potential novel miRNAs using MIREAP software if their precursors could form hairpin structures (Fig. S2). Consequently, 1,310 known miRNAs were detected in PS, TS, and SS, containing 371 existing miRNAs and 939 conserved miRNAs (Table S2). The numbers of the existing miRNAs and conserved miRNAs exhibited differences among PS, TS, and SS, which had 361, 345, and 334 existing miRNAs and 531, 527, and 548 conserved miRNAs, respectively (Fig. 2A). Moreover, we identified 1,727, 1,723, and 1,597 novel miRNAs with high reliability from non-annotated sRNAs of PS, TS, and SS, respectively (Table S3; Fig. 2B). In summary, we identified 2,619, 2,595, and 2,479 miRNAs from PS, TS, and SS containing 361, 345, and 334 existing miRNAs, 531, 527, and 548 conserved miRNAs, 1,727, 1,723, and 1,597 novel miRNAs, respectively (Fig. 2C).

Additionally, we observed that the abundances of the above-identified miRNAs displayed differences among PS, TS, and SS (Table S2). For example, the miRNA family with the highest abundance in PS and TS was the ptc-miR166 family, with 21,349,509 and 8,730,386 TPM, respectively. The ptc-miR319 family with 709,709 TPM was the second-highest abundant miRNA family in PS, while the ptc-miR396 family with 286,019 TPM was the second-highest abundant miRNA family in TS. The ptc-miR396 and ptc-miR319 families, with 5,034,301 and 592,466 TPM, respectively were the highest and second-highest abundant miRNA families in SS, respectively. Moreover, the miRNAs from the same family had distinct expression abundances among PS, TS, and SS (Table S2). For example, the abundances of ptc-miR396a and ptc-miR396b increased from PS to SS, but ptc-miR396c, ptc-miR396d, and ptc-miR396e-5p showed higher abundances in TS than in PS and SS. These results demonstrate that the miRNAs of the same family or different families had different expression patterns among different developmental stems of poplar, suggesting that they could play various roles in diverse phases of wood formation.

Differentially expressed miRNAs and their candidate target genes in diverse developmental stages of *P. trichocarpa* stems

A comparative analysis was performed to identify the differentially expressed miRNAs (DE-miRNAs) involved in diverse developmental phases of wood formation. 114 (36 up-regulated and 78 down-regulated), 306 (76 up-regulated and 230 down-regulated), and 152 (26 up-regulated and 126 down-regulated) DE-miRNAs were identified in PS vs TS, PS vs SS, and TS vs SS, respectively (Fig. 3A ; Tables S4–6).

To identify the target genes of DE-miRNAs by integrated analysis of the miRNA and mRNA expression profiles, we concurrently performed mRNA-seq using the same materials as those for small RNA-sEq. By comparing the expression levels of genes among PS, TS, and SS, we obtained 4,975 (2,113 up-regulated and 2,862 down-regulated), 10,514 (3,467 up-regulated and 7,047 down-regulated), and 4,780 (1,158 up-regulated and 3,622 down-regulated) differentially expressed genes (DEGs) in PS vs TS, PS vs SS, and TS vs SS, respectively (Fig. 3B; Tables S7–9). According to the results of gene function annotation, Gene Ontology (GO) and Kyoto Encyclopaedia of Genes and Genomes (KEGG) analysis, we observed that many of these DEGs were related to different processes and pathways of wood formation (Tables S10–15).

We predicted 921, 2,639, and 2,042 candidate target genes (CTGs) from the above DEGs for 114, 306, and 152 corresponding DE-miRNAs using PatMatch software (Version 1.2), which led to the identification of 158, 855, and 297 significant DE-miRNA-CTG pairs in PS vs TS, PS vs SS, and TS vs SS, respectively (Tables S16–18). Among these pairs, 33, 109, and 107 pairs had a significantly positive correlation and 78, 307, and 119 pairs had no significant correlation, while 47, 439, and 71 miRNA/CTG pairs had a significantly negative correlation with Pearson correlation coefficients varying from − 0.8111 to − 0.995 in PS vs TS, PS vs SS, and TS vs SS, respectively (Tables S16–18, Fig. 3C). The miRNA-CTG pairs comprised 23, 128, and 25 DE-miRNAs and 35, 230, and 65 corresponding CTGs, respectively (Tables S19–21). The significant inverse relationships between DE-miRNAs and their CTGs in profiles indicate these miRNAs exert strongest regulation on these CTGs. Other DE-miRNAs and CTGs, which were in relatively large quantity and did not exhibit significant pairwise inverse relationships, might be subjected to more complicated multiple regulation by multiple miRNAs, and most likely by *TFs*, constituting extremely complicate regulatory relationships and networks in the genome.

Regulatory relationships of DE-miRNA and CTGs

Among the above significantly and negatively related DE-miRNA-CTG pairs, 6, 27, and 6 miRNA families had more than one CTGs, while one, four, and one miRNA family have only one CTG in PS vs TS, PS vs SS, and TS vs SS, respectively (Tables S18–20). For example, in PS vs TS, miR858 and miR9776-x had five CTGs, Potri.T13100, *MYB83* (Potri.001G267300), *MYB52* (Potri.005G186400), *MYB63* (Potri.005G096600), and *MYB35* (Potri.015G067700), about 14.3% of all CTGs (Fig. 4A); in PS vs SS, miR9776-x had 30 CTGs, including *CYCA3;4* (Potri.014G021100), Potri.002G032400, and *IAA14* (Potri.002G044900), accounting for 13.0% of all CTGs (Fig. 4B); miR3946-x had 28 CTGs, including *CRT1*

(Potri.013G060500 and Potri.019G032500), *RLP46* (Potri.001G003200), and *MYB23* (Potri.001G169600), accounting for 43.0% of all CTGs in TS vs SS (Fig. 4C). Additionally, 8, 26, and 11 DE-miRNAs were associated with only one CTG, such as ptc-miR6457b and CTG Potri.003G152300 in PS vs TS, miR4394-y and CTG *TPS5* (Potri.001G139500) in PS vs SS, and novel-m0573-3p and CTG Potri.001G102600 in TS vs SS, respectively (Fig. 4). The lower connectivity of these miRNAs in their regulatory networks suggest that they are not powerful effectors.

Furthermore, multiple DE-miRNAs had one CTG. For example, *RLP21* (Potri.006G061300) was repressed by four members of the ptc-miR-390 family in PS vs TS (Fig. 4A). *HB-15* (Potri.001G188800) was repressed by 19 members of the ptc-miR166 family, ptc-miR5168-y, and ptc-miR165-y in PS vs SS, respectively (Fig. 4B). Additionally, in TS vs SS (Fig. 4C), *HSFB3* (Potri.016G056500) was repressed by novel-m1696-3p, novel-m1328-3p, and novel-m0719-5p. The above results suggest that these DE-miRNAs performed various biological functions through repressing one CTG, multiple CTGs, or multiple DE-miRNAs involved in the same or different biological processes in diverse phases of wood formation.

Functions of DE-miRNAs in diverse phases of wood formation

Generally, the biological functions of miRNAs are manifested through negatively regulating their CTGs by either mRNA degradation or translational suppression based on sequence complementarity with their target(s)[20]. Thus, we deduced the biological functions of these above DE-miRNAs by analysing the functions of their significantly and negatively regulated CTGs. According to the functional annotation of these CTSs, we found 5, 30, and 4 CTGs encoding TFs, which are CTGs of 3, 37, and 6 corresponding DE-miRNAs and formed 6, 142, and 6 DE-miRNA-CTG pairs, in PS vs TS, PS vs SS, and TS vs SS, respectively (Tables S19–21). Some of these *TFs* have been reported to play important roles in diverse phases of wood formation. For example, *IAA14* (Potri.002G044900), which is the miR9776-x CTG and significantly up-regulated in PS compared with that in TS and SS, respectively (Fig. 5), is involved in auxin signal transduction and vascular development by interacting with *ARF5* [30]. Moreover, multiple *TFs* in the CTGs of DE-miRNAs in PS vs SS that were significantly up-regulated in PS compared with those in SS were primarily involved in cell division and expansion, processes in the beginning phase of wood formation. For example, the *SPL2* (Potri.018G149900), *SPL10* (Potri.014G057800), *SPL11* (Potri.002G142400), *SPL3* (Potri.011G055900), and *SPL5* (Potri.011G116800) CTGs of the miRNA156 family have been reported to regulate lateral root growth by directly regulating *AGL79* and shoot development in the vegetative phase [31–34]. ptc-miR172d and ptc-miR172e CTG *AP2* (Potri.005G140700) are involved in cell division and elongation [35]. ptc-miR159c CTG *MYB33* (Potri.009G018700) promotes cell division in the root meristem by accelerating the cell cycle [36]. Additionally, *AGL22* (Potri.007G010800), the CTG of ptc-miR396a and ptc-miR396b, is involved in the transition from the vegetative state to flowering [37]. The miR9776-x CTG *bHLH110* (Potri.002G032400), together with *AtIBH1* and *PRE1*, constitute a tri-antagonistic *bHLH* system and competitively regulates cell elongation under brassinosteroids (BRs), gibberellins (GAs), and developmental phase-dependent signals [38]. In TS, we also found some *TFs* that were up-regulated compared with those in PS or SS and involved in the cell wall modification and SCW biosynthesis processes of the middle phases of wood formation. For example, *MYB83* (Potri.001G267300), the CTG of

miR858-x and miR858-y, has been reported to directly regulate secondary wall biosynthesis [39]. *MYB63* (Potri.005G096600), *MYB52* (Potri.005G186400), and *MYB35* (Potri.015G067700), CTGs of miR858-y, activate lignin biosynthesis [40], participate in SCW biosynthesis in xylary fibres [39], and regulate callose deposition around pollen mother cells [41], respectively (Fig. 5). *MYB5* (Potri.013G056500), a CTG of novel-m0998-5p, can form MYB–bHLH–WDR (MBW) TF complexes together with TT2 and TTG1 to regulate cuticle biosynthetic pathways [42] and activate flavonoid pathway genes, such as *PAL* and *CHS* [43], of which *PAL* encodes the first enzyme of lignin biosynthesis pathway [44]. Additionally, we observed that some *TFs* of DE-miRNA CTGs were up-regulated in SS compared with those in PS or TS and participated in some typical processes of the late phase of wood formation. For example, *SHN2* (Potri.006G253800 and Potri.018G028000), which was the CTG of miR384 that was significantly up-regulated in SS compared with that in PS (Fig. 5), is a top-level master switch in the hierarchical transcriptional regulation network of SCW formation, up-regulating the expression of genes related to cellulose and hemicellulose biosynthesis and repressing the expression of genes involved in lignin biosynthesis and PCD in poplar [45]. *MYB83* (Potri.001G267300), which was the CTG of miR858-x and miR858-y and up-regulated in SS compared with that in PS, is a master switch that regulates multiple downstream *TFs* and structural genes related to SCW biosynthesis and PCD [39, 46]. miR858-y CTG *MYB63* (Potri.005G096600), which was up-regulated in SS compared with that in PS, is a direct target of *MYB46* and functions as a direct transcriptional activator of lignin biosynthesis [39, 46]. miR858-z CTG *MYB52* (Potri.005G186400), which was significantly up-regulated in SS compared with that in PS, is a downstream *TF* of *MYB46* that activates genes involved in SCW biosynthesis [47]. Moreover, we found that some *TFs*, up-regulated in SS compared with those in TS, are related to various processes of the late phases of wood formation. For example, miR6425-x CTG *ARF7* (Potri.006G077800) indirectly regulates cell wall synthesis and remodelling by activating *MUS* and *MUL*, two kinase-inactive RLKs, under auxin [48]. *MYB23* (Potri.001G169600), a CTG of miR3946-x, is a homologous gene of *MYB52* and plays roles in regulating cuticle biosynthetic pathways[42]. *HB-15* (Potri.001G188800 and Potri.003G050100), a CTG of the miR165-y, miR5168-y and miR166 family, up-regulates genes involved in cellulose biosynthesis and down-regulates lignification- and metabolite-related genes (putative laccase, cinnamoyl CoA reductase, chalcone synthase, putative pectin methyltransferases and pectin esterase)[18, 49]. *HB-8* (Potri.018G045100), a CTG of the miR165-y and miR166 families, promotes vascular cell differentiation and increases the production of lignified tissues[50]. Additionally, we found that *MYB93* (Potri.002G096800), a CTG of novel-m1344-3p, and *HSFs* (Potri.016G056500), CTGs of novel-m0719-5p, novel-m1328-3p and novel-m1696-3p, were up-regulated in SS compared with those in TS, while the functions of these *TFs* in wood formation remain unknown.

Moreover, we found that some CTGs of DE-miRNAs were structural genes related to diverse processes of wood formation. For example, the miR9776-x CTG *CYCA3;4* (Potri.014G021100), miR393 family CTG *T1R1* (Potri.014G134800 and Potri.002G207800), and ptc-miR390a CTGs, *BAM3* (Potri.001G073600), *ICDH* (Potri.010G176000), and *BRL2* (Potri.010G101100), which have been reported to participate in cell division, expansion, and differentiation, respectively[51–54], were significantly up-regulated in PS compared with those in SS or TS (Fig. 6). ptc-miR6441 CTG *PMR5* (Potri.001G278300), which affects

pectin composition[55]; novel-m0058-3p CTG *CRA1* (Potri.005G224700), which regulates lignification and flavonoid production [56], and miR5248-x CTG *DUF642* (Potri.003G059800), which is a pectin methyl esterase and contributes to the modification of cell wall properties[57], were up-regulated in TS compared with those in PS or SS (Fig. 6). Furthermore, novel-m0260-5p CTG *C4H* (Potri.018G146100), novel-m1190-3p CTG *LAC2* (Potri.009G156600 and Potri.009G156800), and miR397-x CTGs *LAC7* (Potri.016G107500 and Potri.006G094100) and *LAC11* (Potri.009G102700) related to lignin biosynthesis and deposition [58–60], miR6425-x CTG *ADF6* (Potri.002G038800) involved in the processes of cellulose elongation and SCW formation during fibre development [61], novel-m0738-5p and novel-m1395-5p CTG *BEN1* (Potri.002G147700, Potri.002G148000, Potri.T168400, Potri.T168500, and Potri.T175100), novel-m1156-3p CTG *XBAT33* (Potri.015G141400), novel-m0112-5p CTG *ABCG40* (Potri.003G183200 and Potri.003G179000), and novel-m1556-3p CTG *RPP4* (Potri.019G098800) involved in PCD[62–65], were up-regulated in SS compared with those in PS or TS (Fig. 6).

We also found that the functions of some DE-miRNAs have not been clarified to date in wood formation, although their expression levels exhibited extreme alternations among PS, TS, and SS (Tables S19–21), suggesting these DE-miRNAs might play roles in specific phases of wood formation. For example, miR858-x and novel-m1201-5p were significantly down-regulated in PS compared with those in TS and SS, respectively, with their corresponding CTGs Potri.T131300 and Potri.010G088200 showing contradictory changes. The expression levels of miR9776-x and ptc-miR172d and their corresponding CTGs Potri.001G062100 and Potri.009G009100 showed significant reverse alternations in TS compared with those in PS and SS, respectively. However, the functions of these miRNAs in different phases of wood formation require further study.

To further determine the biological roles of the above DE-miRNAs in wood formation, we also performed GO and KEGG analyses of their corresponding CTGs in PS vs TS, PS vs SS, and TS vs SS, respectively. As shown in Fig. 7 and Tables S22–24, some significantly enriched biological processes in PS vs TS were the typical processes of the beginning and middle phases of wood formation. For example, ‘photosynthesis’ (GO:0015979), ‘transmembrane transport’ (GO:0055085), and ‘response to stimulus’ (GO:0050896) are involved in the cell division and differentiation of the meristem [66–72], while the ‘oxidation-reduction process’ (GO:0055114) is involved in the synthesis of cellulose [73, 74] (Fig. 7; Table S22). In PS vs SS, some significantly enriched processes, such as ‘photosynthesis, light harvesting’ (GO:0009765) [66–68] and ‘response to temperature stimulus’ (GO:0009266) [70–72], were the typical processes of the beginning phase of wood formation (Fig. 7; Table S23), while the ‘proline metabolic process’ (GO:0006560), ‘cell wall macromolecule catabolic process’ (GO:0016998), and ‘oxidation-reduction process’ (GO:0055114) were the processes of the middle and late phases of wood formation and features of the cell in SS, respectively, as previously reported [73–75]. Among these significantly enriched processes in TS vs SS (Fig. 7; Table S24), ‘proteolysis’ (GO:0006508), ‘nucleic acid metabolic process’, and ‘PCD’ (GO:0012501) were the typical processes of the late phase of wood formation and features of the cells in SS [76].

The results of KEGG analysis showed multiple significantly enriched pathways related to typical pathways of the different phases of wood formation in the PS vs TS, PS vs SS, and TS vs SS, respectively (Table S25). In PS vs TS, 'Plant hormone signal transduction (ko04075)' and 'Photosynthesis-antenna proteins (ko00196)' are related to cell division and differentiation activity[66–68, 77], which were the typical pathways of cells in the beginning phase of wood formation. We also found that some significantly enriched pathways in PS vs SS were typical pathways of the late phase of wood formation (Table S25), such as 'Phenylalanine metabolism (ko00360)' related to cell wall lignification[78], 'Biosynthesis of secondary metabolites (ko01110)' implicated in cellulose and lignin biosynthesis [79, 80], and 'Flavonoid biosynthesis (ko00941)' involved in cell wall stabilization [81], while 'Photosynthesis-antenna proteins (ko00196)' was the typical pathway of the beginning phase of wood formation (Table S25). Additionally, we obtained some significantly enriched pathways belonging to the middle and late phases of wood formation in TS vs SS. For example, 'Glycine, serine and threonine metabolism (ko00260)', which is reported to be related to cell wall synthesis and cell wall remodelling pathways[82], was the typical pathway in the middle phase of wood formation, while the 'Biosynthesis of secondary metabolites (ko01110)' and 'Phenylalanine metabolism (ko00360)' are typical pathways in the late phase of wood formation[78–80].

Together, these results demonstrate that the DE-miRNAs of PS vs TS, PS vs SS, and TS vs SS played various roles in the diverse phases of wood formation by regulating CTGs, which are regulators and structural genes involved in diverse biological processes and pathways of wood formation.

Validation of miRNAs and their CTG expressions using RT–PCR

To validate the expression levels of miRNAs obtained using small RNA-seq and their expression dynamics among PS, TS, and SS, the expression levels of eight known miRNAs (miR9776-x, ptc-miR156g, miR858-y, miR5248-x, ptc-miR166l, miR171-y, ptc-miR393a-5p, and ptc-miR390d-5p) and 5 novel miRNAs (novel-m0058-3p, novel-m1190-3p, novel-m0260-5p, novel-m1556-3p, and novel-mm1156-3p) were analysed by qRT–PCR using the same RNA sources as those for small RNA-seq analysis. The relative transcript levels of these examined miRNAs by qRT–PCR showed good agreement with those obtained by small RNA-seq (Fig. 8A). Moreover, there was a significant regression line with R^2 equal to 0.95 between miRNA expression values obtained by qRT–PCR and small RNA-seq (Fig. 8C), indicating that the expression values of miRNA obtained from two analysis methods were in good agreement. These results confirmed the robustness and reliability of the small RNA-seq results.

To confirm the negative correlations between the miRNAs and their CTGs obtained by integrated analysis of the small RNA and mRNA profiles, the expression levels of the CTGs of miRNAs in PS, TS, and SS were also investigated by qRT–PCR. The expression levels of *IAA14* (Potri.002G044900), *CYCA3;4* (Potri.014G021100), *SPL2* (Potri.018G149900), *SPL10* (Potri.014G057800), *TIR1* (Potri.014G134800), *MYB83* (Potri.001G267300), *MYB52* (Potri.005G186400), *HB-8* (Potri.018G045100), *HB-15* (Potri.001G188800), *LAC2* (Potri.009G156600), *XBAT33* (Potri.015G141400), *ICDH* (Potri.010G176000), *CRA1* (Potri.005G224700), *DUF642* (Potri.003G059800), *RPP4* (Potri.019G098800), and *C4H*

(Potri.018G146100) exhibited opposite trends to the corresponding miR9776-x, ptc-miR156g, ptc-miR393-5p, miR858-y, ptc-miR166l, novel-m1190-3p, novel-m1156-3p, ptc-miR390d-5p, novel-m0058-3p, miR5248-x, novel-m1556-3p, and novel-m0260-5p in PS, TS, and SS, respectively (Fig. 8A and B). However, we also found that the expression levels of miR171-y and CTG *MYB42* (Potri.001G118800) exhibited the same change trend from PS to SS (Fig. 8A and B), suggesting a positive correlation between this miRNA-CTG pair and demonstrating the presence of other regulators such as *MYB46* [83], together with miRNA, potentially involved in controlling the expression of *MYB42*. Together, these results also demonstrated that the identified miRNAs involved in the diverse phase of wood formation were generally negatively related to their CTGs.

3 Discussion

Wood formation comprises several continuous biological processes[1] that require multiple molecular regulatory mechanisms to synergistically regulate the expression of many genes related to various processes of wood formation[5, 8, 39]. Although numerous miRNAs involved in the regulation of specific biological processes in wood formation have been identified thus far [12–18], how many miRNAs exist and the molecular functions these miRNAs in the diverse processes of wood formation remain unclear. The vertical segments of the less than one-year-old poplar that include all processes of wood formation and that can be divided into three phases—beginning, middle, and late phases of wood formation[25, 26]—have been used to investigate the dynamics of the molecular regulatory mechanisms underlying diverse phases of wood formation [26]. In the present study, to uncover the dynamics of miRNAs and their biological functions underlying diverse phases of wood formation, we performed integrated analysis of the mRNA and small RNA expression profiling of PS, TS, and SS in less than one-year-old poplar trunks by Solexa sequencing.

miRNA length and expression variation among diverse phases of wood formation

Through small RNA high-throughput sequencing technology, we generated 15,687,101, 15,980,089, and 1,226,233 reads from PS, TS, and SS libraries and finally identified 12,237,495, 11,639,629, and 9,336,272 sRNAs, respectively (Table 1). These results demonstrate that the *P. trichocarpa* woods during diverse phases contain large and diverse sRNA populations, a finding similar to previous study findings in *P. balsamifera* [84] and Chinese fir [85]. Moreover, we observed that 21-nt sRNAs were the most numerous, comprising approximately 56.25% of the total sRNAs, with 24-nt sRNAs being the second most frequent, averaging approximately 14.8%. These distribution patterns of sRNA lengths in diverse phases of wood formation in *P. trichocarpa* were also found in grapevine [86], cotton[87], Chinese white poplar [88], and Norway spruce (*Picea abies*) [89]. However, it was notable that the abundances of 21- and 24-nt sRNAs exhibited significant differences among PS, TS, and SS,. The differences in the 21- and 24-nt sRNA abundances were also observed in *P. tomentosa* under phosphate starvation [90], different development states of cambium in *Cunninghamia lanceolate* [85], and between angiosperms and gymnosperms [85]. These results demonstrate that the lengths of sRNAs and abundances of major sRNAs vary among plant species, developmental states, and tissues of the same plant.

Because most plant sRNAs are produced as 21- to 24-nt RNA molecules due to the activities of Dicers (*DCLs*), Argonautes (*AGOs*), RNA-dependent RNA polymerases (*RDRs*), and SUPPRESSOR OF GENE SILENCING2/3 (*SGS2/3*)[91, 92], we suspected differences in the expression of the above genes among PS, TS, and SS. We observed that the expression of *DCL4* (Potri.006G188800), *DCL2* (Potri.008G075900 and Potri.010G181400), *RDR2* (Potri.015G073700), *AGO4* (Potri.006G025900), *AGO6* (Potri.014G159400), *AGO5* (Potri.009G001500 and Potri.001G213700), *AGO10*(Potri.010G081300 and Potri.008G158800), *AGO7* (Potri.010G163800), *AGO2* (Potri.012G118700 and Potri.015G117400), and *SGS3* (Potri.003G187900, Potri.003G188100, and Potri.003G188200) obviously varied among PS, TS, and SS (Tables S7–9). However, no consistencies were found between the expression abundances of the above genes and those of 21- to 24-nt RNA molecules among PS, TS, and SS. We speculated that these genes might have post-transcription or post-translation modifications. Interestingly, *AGO2* (Potri.015G117400) was found to be regulated by miR1167-y in PS vs SS. In summary, these results further demonstrate significant differences in the molecular mechanism of the sRNA biogenesis pathways among diverse phases of wood formation.

miRNAs identified from diverse phases of wood formation

We identified 892 (361 existing miRNAs and 531 conserved miRNAs), 872 (345 existing miRNAs and 527 conserved miRNAs), and 882 (334 existing miRNAs and conserved miRNAs) known miRNAs from 491, 478, and 503 miRNA families, and 1,727, 1,723, and 1,597 novel miRNAs in PS, TS, and SS, respectively (Fig. 2C). Among these miRNAs, nine conserved miRNAs, such as miR9776, miR7741, miR6265, and miR4394 (Table S26), had not been previously reported in *Populus* or other plant species, and 760 miRNAs, such as miR8664-y, miR7729-y, miR6277-y, and miR5815-x, belonged to low-expression miRNAs (TPM < 1) (Table S2). These results also demonstrate that the small RNA high-throughput sequencing approach is suited for identifying more species-specific miRNAs or miRNAs with very low expression in plants. Additionally, we found that only 56 (2.14%), 58 (2.24%), and 55 (2.22%) miRNAs showed TPM > 1000 on average, accounting for 99.65%, 99.26%, and 98.56% of the total TPM of miRNAs in PS, TS, and SS, respectively (Tables S2–3). These results were consistent with those of previous reports that the plant small RNAs primarily comprise many miRNAs with low-level expression and few miRNAs with high-level expression[20].

miRNA/mRNA pairs of diverse phases of wood formation

Plant miRNAs only have a few mRNA targets [93]. However, our data demonstrated 1,867 (921, 2,639, and 2,042) CTGs, targets of 190 (114, 306, and 152) DE-miRNAs on average in poplar stems (PS, TS, and SS), approximately 4% of the protein-coding genes of poplar and greater than approximately 1% and 3% of the protein-coding genes in subcultured *Taxus* cells and *Arabidopsis*, respectively [93, 94]. These results indicate that our miRNA data had excellent coverage.

We predicted 158, 855, and 297 DE-miRNA-CTG pairs between the 114, 306, and 152 DE-miRNAs and 921, 2,639, and 2,042 corresponding CTGs in PS vs TS, PS vs SS, and TS vs SS, respectively (Fig. 3A and B; Tables S4–9). Among these DE-miRNA-CTG pairs, 47, 439, and 71 pairs showed a significantly negative

correlation, 33, 109, and 107 pairs showed a significantly positive correlation, and 78, 307, and 119 pairs showed no significant correlation, representing 42.5%, 22.4%, and 35.5% of the total DE-miRNA-CTG pairs on average, respectively (Tables S16–18). These results demonstrate that the negatively related DE-miRNA-CTG pairs numbered about twice as high as the positively related pairs, a finding that is not consistent with the findings in *Taxus* and the tomato [94, 95], suggesting the differently related miRNA-mRNA pairs vary among plant species or different tissues of the same plant. Additionally, because a gene can be regulated by multiple regulatory factors, the inhibitory effects of an miRNA on its target gene can be attenuated or masked by other regulatory factors; thus, the relationship between a miRNA and target gene does not necessarily show a negative correlation. For example, *LAC4* is not only repressed by ptr-miR397a but also activated by *MYB58* and *MYB63* in poplar [13]. In the present study, perhaps due to the *MYB46* and *MYB83* activating effects on *MYB42* [39, 83], miR171-y and its target gene *MYB42* (Potri.001G118800) exhibit a positive correlation.

Although these DE-miRNAs with non-negative relation of their CTGs could function in the biological processes of plants according to a previous report [96], the functions of these DE-miRNAs could not be determined because their target genes were not accurately identified by integrated analysis of the miRNA and mRNA expression profiles due to the interference effects of other regulatory factors. Thus, in the present study, we did not further analyse these positively or not significantly related DE-miRNA-CTG pairs and only focused on the significantly negatively related DE-miRNA-CTG pairs. Notably, these negatively related DE-miRNA-CTG pairs comprised 23, 128, and 25 DE-miRNAs, and 35, 230, and 65 corresponding CTGs (Tables S19–21), representing only 20.17%, 41.83%, and 16.45% of the total DE-miRNAs and 0.70%, 2.19%, and 1.36% of the total DEGs in PS vs TS, PS vs SS, and TS vs SS, respectively. These results suggest that miRNA regulation probably accounts for a small part of the molecular regulatory mechanisms underlying diverse phases of wood formation.

Functions of previously identified miRNAs in diverse phases of wood formation

Previous studies in tree species have revealed that miRNAs are implicated in multiple biological processes of plant growth and development by regulating their target genes [97]. In the present study, we also revealed that multiple miRNAs, which have been reported previously to play important roles in multiple processes of plant growth and development, are involved in different phases of wood formation. For example, the miRNA156 family was significantly down-regulated in PS compared with that in SS, suggesting that the miRNA156 family participated in the beginning phase of wood formation by alleviating their inhibitory effects on target *SPLs* related to activating cell division (Fig. 9)[31–34]. miR156 regulates cell division and elongation by down-regulating the *SPL* family in vascular cambium transition from dormancy to the active growth phase in *Cunninghamia lanceolate* [98] and the juvenile-to-adult transition in *Arabidopsis* and maize [99, 100]. Additionally, miRNA156 is involved in lateral root growth and is responsive to auxin signalling by repressing *SPLs* in *Arabidopsis* [101]. These results revealed that the miRNA156 family participates in multiple biological processes of plant growth and development by regulating different *SPLs*. ptc-miR172d and ptc-miR172e were observed to be involved in the beginning phase of wood formation by significantly reducing the inhibition effects on target *TFs AP2*

(Potri.005G140700) and *AP2 TF RAP2.7* (Potri.006G132400 and Potri.016G084500) (Fig. 9), which activate cell division and elongation[35], in PS compared with those in SS. The functions of ptc-miR172d and ptc-miR172e in the present study were somewhat similar to that of cln-miR172, which regulates cell division and elongation by alleviating the inhibitory effect on its target *TF AP2* in the transition from the dormancy of vascular cambium in *Cunninghamia lanceolate* [98], but was different from that of miR172 in *Arabidopsis*, being involved in the autonomous flowering pathway by regulating its target *TF TOE1* [102]. These results suggest that miR172 may be involved in multiple biological processes in plant growth and development by regulating the same or different target *TFs*. We found that miR159c was significantly down-regulated, and its target *MYB33* (Potri.009G018700) was strongly up-regulated, in PS compared with those in SS, alleviating the miR159c inhibitory effects on its target *TF MYB33*, which can activate cell division[36]. This result demonstrated that miR159c was involved in the beginning phase of wood formation (Fig. 9), a finding that is similar to a previous study finding that miR159 facilitates the vegetative phase change by regulating its target *TF MYB33*, which promotes cell division by promoting *SPL9* expression in *Arabidopsis thaliana* [103]. miR396 functions in cell division, differentiation, proliferation, and elongation mainly by regulating *GRFs*/ *GIFs* in the leaf size and vegetative phase transition, shoot and shoot lateral organ growth, floral organ development, and the response to abiotic and pathogen stress [104]. In the present study, ptc-miR396a and ptc-miR396b were identified to participate in the beginning phase of wood formation by regulating its target *TF AGL22* (Potri.007G010800) related to activating the cell division process (Fig. 9) [37]. These results demonstrated that miR396 plays different roles in different plant species or plant tissues by regulating different target *TFs*. We also found that miR393-x, miR393b-5p and miR393a-5p are significantly down-regulated and their target *TIR1* (Potri.002G207800) is strongly up-regulated in PS compared with that in SS, indicating that miR393 in poplar is involved in the beginning phase of wood formation by alleviating the inhibitory effects on *TIR1* related to activating cell division (Fig. 9) [9], a finding that is somewhat consistent with the result that miR393a inhibits shoot regeneration by repressing *TIR1* in the de novo formation of SAM [105].

MiR858 can regulate *MYB81*, *MYB97*, *MYB120*, *MYB65*, and *MYB104* orthologs in *Salvia miltiorrhiza* [106], a negative regulator of anthocyanin biosynthesis, by repressing the target *AaMYBC1* in red-coloured kiwifruit [107], mediating the cleavage of *SlMYB7-like* and *SlMYB48*-like *TFs* in *Solanum lycopersicum* [108], regulating *VvMYB114* to promote anthocyanin and flavanol accumulation in grapes[109], regulating the homologous *MYB2* gene in *Arabidopsis* trichome and cotton fibre development[110], and interfering with the *Heterodera schachtii* parasitism of *Arabidopsis* by repressing *MYB83* [111]. In the present study, we found that miRNA858s participated in the SCW biosynthesis of the middle and late phases of wood formation by significantly alleviating the inhibitory effects on the target *TFs MYB52* (Potri.005G186400), *MYB83* (Potri.001G267300), and *MYB63* (Potri.005G096600) in TS and SS compared with those in PS, respectively. To our best knowledge, this report is the first to identify miRNA858s as being involved in wood formation by regulating the key *TFs* (*MYB52*, *MYB83* and *MYB63*) of the transcriptional regulation network of secondary wall formation (Fig. 9)[3, 39]. These results also

demonstrated that miRNA858s participate in multiple biological processes by regulating different target genes among different plant species.

HB-8 and *HB-15* play potential roles in xylem formation and are regulated by only one miRNA, miR166, in *Acacia mangium*[112]. However, we observed that, when *HB-8* (Potri.018G045100) and *HB-15* (Potri.001G188800 and Potri.003G050100) participated in the biological processes of the late phase of wood formation of poplar (Fig. 9), such as cellulose biosynthesis and lignification [18, 49, 50], they were regulated by not only the miR166 family but also the miR165-y and miR5168-y (Fig. 9). These results demonstrated different miRNA regulatory mechanisms of *HB-8* and *HB-15* involved in wood formation among different plant species. In a previous study, miR397 functions in the lignification of wood formation by regulating 29 *LACs* of the *LAC* family in poplar [13]. We found that miR397s, including ptc-miR397a and miR397-x, were involved in the lignification process of the late phase of wood formation only by regulating two target genes, *LAC7* (Potri.016G107500, Potri.006G094100) and *LAC11* (Potri.009G102700) (Fig. 9). The difference in the number of target genes of miR397 might be caused by different miRNA identification methods or research material differences between the present and previous studies of poplar.

Functions of the first identified miRNAs participate in diverse phases of wood formation

In addition to the above-described miRNAs, we also identified multiple miRNAs that are have not been reported to be related to wood formation. For example, we found that miR9776-x participated in the beginning phase of wood formation by significantly alleviating the inhibitory effects on the target *TF IAA14* (Potri.002G044900) and structural gene *CYCA3;4* (Potri.014G021100), which activate cell division, expansion, and differentiation processes [30, 54], in PS compared with those in TS and SS(Fig. 9). ptc-miR390a might play roles in the beginning phase of wood formation by significantly alleviating the inhibitory effects on target structural genes *BAM3* (Potri.001G073600), *ICDH* (Potri.010G176000), and *BRL2* (Potri.010G101100) (Fig. 9), which have been reported to be related to cell division, expansion, and differentiation[113–115], in PS compared with those in TS and SS.

In the middle and late phases of wood formation, we found that miR858-y might function in lignin biosynthesis and callose deposition processes by significantly alleviating the inhibitory effects on *TFs MYB63* (Potri.005G096600) [3, 39] and *MYB35* (Potri.015G067700) [41] that caused their significant up-regulation in TS and SS compared with those in PS (Fig. 9). miR3946-x and novel-m0998-5p were found to function in the late phase of wood formation by significantly alleviating the inhibitory effects on target *TFs MYB23* (Potri.001G169600) and *MYB5* (Potri.013G056500) related to cuticle biosynthetic of cell wall [42] by their expression being significantly decreased in SS compared with those in TS (Fig. 9). miR6425-x was found to be involved in the late phase of wood formation by significantly alleviating the inhibitory effects on the target *TF ARF7* (Potri.006G077800) (Fig. 9), which activates cell wall synthesis and remodelling processes[48], in SS compared with those in PS. Most notably, we found that miR384-x regulated *SHN2* (Potri.018G028000 and Potri.006G253800), which is a high hierarchical master switch *TF* that appears to control the switch between cellulose and lignin biosynthesis [45], suggesting that

miR384-x participates in multiple biological processes, such as secondary wall biosynthesis, lignification, and PCD, of the middle and late phases of wood formation (Fig. 9).

Moreover, we found miRNAs involved in the middle and late phases of wood formation that regulate structural genes related to wood formation. For example, miR5248-x was involved in the middle phase of wood formation by regulating *DUF642* (Potri.003G059800) related to the modification of cell wall properties (Fig. 9)[57]. ptc-miR6441 participated in the late phase of wood formation by alleviating the inhibitory effects on *PMR5* (Potri.001G278300) related to the regulation of pectin composition (Fig. 9) [55]. miR6425-x was identified to participate in the late phase of wood formation by alleviating the inhibitory effect on the target gene *ADF6* (Potri.002G038800) (Fig. 9), whose homologous gene *ADF3* plays a critical role in the processes of elongation and SCW formation during fibre development[61]. *C4H* (Potri.018G146100), a key gene in the lignin biosynthesis pathway [116], was first identified to be regulated by novel-m0260-5p, which was significantly down-regulated in SS compared with that in PS, suggesting novel-m0260-5p regulates lignin biosynthesis in the late phase of wood formation (Fig. 9). novel-m0058-3p was involved in the late phase of wood formation by alleviating the inhibitory effects on the target gene *CRA1* (Potri.005G224700) related to the regulation of lignification and flavonoid production (Fig. 9) [56]. In addition to the previously identified miRNAs, miR397 and ptc-miR397 [13], of *LACs*, we also identified a new regulatory miRNA of *LAC*, novel-m1178-5p (Fig. 9), which targeted *LAC2* (Potri.009G156800, Potri.009G156600) in SS; thus, it functioned in the late phase of wood formation.

Moreover, we first identified some miRNAs related to the PCD process in the late phase of wood formation. For example, the expressions of novel-m1395-5p, novel-m0738-5p, novel-m1156-3p, novel-m0112-5p, and novel-m1556-3p were significantly deceased in SS compared with that in PS and TS, respectively, strongly alleviating the inhibitory effects on their corresponding target genes *BEN1* (Potri.002G147700, Potri.002G148000, Potri.T168400, Potri.T168500, and Potri.T175100), *XBAT33*(Potri.015G141400), *ABCG40* (Potri.003G183200 and Potri.003G179000), and *RPP4* (Potri.019G098800) related to PCD as reported previously [58–60, 62–65], suggesting novel-m1395-5p, novel-m0738-5p, novel-m1156-3p, novel-m0112-5p, and novel-m1556-3p regulated the PCD process in the late phase of wood formation (Fig. 9).

Conclusion

Our study identified a battery of miRNAs including both known and many novel ones involved in diverse phases of wood formation varying from predominantly primary to secondary growth, and then interactively analysed the miRNAs and mRNA expression profiles across diverse developmental stems of *P. trichocarpa*, shedding some lights on many dynamic and diversified aspects, and details of miRNA regulation during vegetative growth to secondary wood formation. Our results demonstrated that miRNAs not only regulate some important *TFs* but also structural genes directly and indirectly involved in diverse processes of wood formation, suggesting that further studies of wood formation should also focus on miRNAs in order to obtain a holistic picture of the underlying molecular regulatory mechanisms. There are still a number of miRNAs with novel functions that need to be characterized. To our knowledge, this study

is the first systematic investigation of miRNAs and their targets involved in diverse phases of wood formation using integrated analysis of miRNA and mRNA expression profiles. The copious information and data provided here will advance the roles of miRNAs and their regulatory functions in diverse phases of wood formation in tree species.

4 Methods

Plant material and RNA extraction

A few plantlets of *P. trichocarpa* clone Nisqually-1, whose genome was sequenced early, were obtained from the Shanghai Institute for Biological Sciences, Chinese Academy of Sciences, and vegetatively propagated in our lab using tissue culture [117]. The plantlets were planted in humus soil and grown under 16 h/8h day/night photoperiod at 25 °C in the greenhouse at Northeast Forestry University for 90 days. The lengths of all internodes (IN) from the apical buds to the bases of the main stems of all trees were measured. The IN2, IN4, and IN8 internodes were PS, TS, and SS stages from primary growth to secondary growth of poplar and represent the beginning, middle, and middle and late phases of wood formation for high-throughput sequencing, respectively. Then, Wang et al. used 63 trees as experimental materials for transcriptome and small RNA sequencing and qRT-PCR analysis. These materials were sampled and immediately frozen in liquid nitrogen and stored at -80 °C following our previous study[28].

RNA extraction, library construction, and small RNA sequencing

Total RNA was extracted using Trizol (Invitrogen) according to the manufacturer's protocol, and the quantity and integrity of RNA were examined using a 2100 Bioanalyzer with the RNA 6000 Nano Kit (Agilent Technologies, Santa Clara, CA, USA). Sequencing libraries were generated using NEBNext® Multiplex Small RNA Library Prep Set for Illumina® (NEB, USA.) following manufacturer's recommendations. All the nine libraries from the three groups were for sRNA sequencing using Illumina Solexa Genome Analyzer II was according to the manufacturer's protocol (Illumina, San Diego, CA, USA).

Transcriptome sequencing and gene expression analysis

The same plant materials used for small RNA sequencing were also for transcriptome sequencing. The materials were first ground to powder in liquid nitrogen and total RNA was isolated using an RNA isolation kit (Auto Lab Biotechnology, Beijing, China). Using the RNase-Free DNase Set (Qiagen), we performed on-column DNase digestions three times during the RNA purification. The quantity and quality of extracted RNA were determined with a NanoDrop ND-1000 (Thermo, USA).

Whole transcriptome libraries were constructed using the NEB Next Ultra Directional RNA Library Prep Kit for Illumina (NEB, Ipswich, MA, USA) according to the manufacturer's instructions; the resulting libraries were assessed for size, quantitation, integrity and purity using a Bioanalyzer 2100 system and qPCR (Kapa Biosystems, Woburn, MA, USA). The libraries with good quality were subsequently sequenced on a HiSeq 2500 instrument that was set to produce 125 bp paired-end reads of 125 nucleotide long. Raw

sequences were cleaned as follows: 1) remove reads containing adapters; 2) remove reads containing more than 10% unknown nucleotides (N); 3) remove low quality reads containing more than 50% low quality (Q-value ≤ 20) bases. After that, the clean reads from all the samples were mapped to the *P. trichocarpa* genome using Bowtie2 and TopHat2 software with default parameters. The expression levels of the protein-coding genes were calculated and normalized using fragments per kilobase of gene per million mapped fragments (FPKM) by Cufflinks (version 2.2.1).

Analysis of small RNA sequencing data

From the raw sequence reads obtained from the small RNA sequencing, we first removed low quality reads, including those shorter than 18 nt or longer than 30 nt, those with more than 10 nt single nucleotide repeats, or more than 10% N, and those with 5' adapter contaminants, or without a 3' adapter or the insert tag. Then the 3' and 5' adapters were removed to obtain clean reads without any mismatches, which were mapped to *P.trichocarpa* genome (https://phytozome-next.jgi.doe.gov/info/Ptrichocarpa_v3_0) using bowtie software (http://sourceforge.net/projects/bowtie-bio/files/) without any mismatch.

Small RNA reads annotation and miRNA identification

All mapped reads were annotated as follows. First, the small RNA were annotated in the GenBank (http://www.ncbi.nlm.nih.gov/genbank/) and Rfam (11.0 release, http://rfam.xfam.org/) database, then the non-coding RNAs, i.e., tRNAs, rRNAs, scRNAs, snRNAs, and snoRNAs, were discarded from the small RNA sequences. Subsequently, the Repeat Masker was used to remove the repeat-associated RNAs (Repbase v.18.07, http://www.girinst.org/). Finally, the remaining sequences which exactly matched the mRNA were analyzed by a BLAST search against miRBase (Release 22) to identify the known miRNAs. The perfectly matched with *P. trichocarpa* miRNA sequences were considered to be the existing miRNAs. And the matched with other plant miRNA sequences were considered to be the conserved miRNAs

The remaining reads were used to predicate novel miRNAs were predicted using MIREAP (http://sourceforge.net/projects/mireap/), based on secondary structure, the Dicer cleavage site, and the minimal folding free energies [118].

Identification of DE-miRNAs and DEGs

Differentially expressed miRNAs (DE-miRNAs) among PS, TS, and SS were identified with edgeR package using the abundance of transcript per million (TPM). The miRNA frequency from the three types libraries was normalized respectively to get the abundance of transcript per million (TPM): normalized miRNA expression = (actual miRNA count/total count of clean reads) × 1,000,000. The abundance changes among PS, TS, and SS were calculated as log2 (TS/PS, SS/PS, or SS/TS). miRNAs with an absolute $|\log2(FC)| \geq 1$ and a *p*-value ≤ 0.05 were thought to be changed significantly and were considered as DE-miRNA.

Differentially expressed genes (DEGs) among PS, TS, and SS were also identified with edgeR package using the FPKM value. Genes exhibiting difference of $|\log2(FC)| \geq 1$ with FDR ≤ 0.05 were considered as differentially expressed.

miRNA target gene prediction

The candidate target genes (CTGs) of DE- miRNAs were predicted by using software PatMatch (Version 1.2) blasting against their corresponding DEGs of PS vs TS, PS vs SS, and TS vs SS comparison, respectively, abiding by rigorous parameters as follows: No more than four mismatches between sRNA/target (G-U bases count as 0.5 mismatches); No more than two adjacent mismatches in the miRNA/target duplex; No adjacent mismatches in positions 2–12 of the miRNA/target duplex (5' of miRNA); No mismatches in position 10–11 of miRNA/target duplex; No more than 2.5 mismatches in position 1–12 of the miRNA/target duplex (5' of miRNA); Minimum free energy (MFE) of the miRNA/target duplex should be ≥ 74% of the MFE of the miRNA bound to it's perfect complement.

Correlation analysis between the DE-miRNAs and their CTGs

Analysis to identify correlations between DE-miRNA and CTG expression in PS vs TS, PS vs SS, and TS vs SS comparison were done using an inhouse R script, respectively. Then for each DE-miRNA, Pearson correlation coefficients were computed for its predicted CTGs, and a contingency Table was created for all CTGs, which was used to assess the level of the negative correlated CTGs (correlation < 0 and *p*-value of correlation ≤ 0.05) within predicted CTGs of the intended DE-miRNA.

GO enrichment and KEGG pathway analysis

To improve elucidation of the potential DE-miRNA regulatory roles, CTGs of DE-miRNAs to a gene ontology (GO) analysis, which were performed using Gene Ontology (GO, http://www.geneontology.org/). Putative CTGs related to metabolism in the cellular processes group were analyzed and annotated according to the Kyoto Encyclopedia of Genes and Genomes (KEGG) database (http://www.genome.jp/kegg/kegg1.html). Pathway enrichment and categorization were performed using the KEGG and GO databases with corrected $p \leq 0.05$ as a threshold.

DEGs among PS, TS, and SS comparison were also performed GO and KEGG analysis, respectively.

Real-time quantitative PCR analysis of miRNAs and CTGs

Total RNA was isolated from the same materials of PS, TS, and SS used to small RNA and expression profile sequencing with RNAiso plus (Takara, China) according to the manufacturer’s instructions. The first cDNA strand was synthesized from total RNA using the TransScript miRNA-reverse transcriptase (RTase) (Trans, China) and miRNA specific stem-loop primers were designed according to the method described by Chen et al.[119]. Briefly, six nucleotides that paired with the 3’ end of the miRNA were linked to a stem-looped sequence (GTCGTATCCAGTGCAGGGTCCGAG GTATTCGCACTGGATACGAC) to synthesize the stem-loop reverse transcription primer. For target genes, the first cDNA strand was

synthesized from total RNA using the TransScript RT/RI RTase (Trans, China). The next steps were identical to the reverse transcription of miRNA.

The expression change levels of miRNAs or CTGs were assessed on an ABI 7500 Fast Real-Time PCR instrument (Applied Biosystems, USA) with TransStart Top Green qPCR SuperMix (Trans, China), and the 5.8S rRNA gene was used as a as the endogenous reference. For target genes, the *β-actin* was selected as reference gene for normalization. $2^{-\Delta\Delta CT}$ relative quantification method was used to analyze the relative changes of miRNAs and their targets expression in qPCR experiments [120]. All of the qPCR reactions were conducted in three replicates. Standard errors and standard deviations were calculated from replicates.

Data analysis

The data were analyzed standard errors and standard deviations using SPSS 21 (Chicago, IL, USA). A statistically significant level was set to a p-value ≤ 0.05. The data are presented as mean ± standard error (SE) with each SE being calculated from three independents biological samples.

5 Abbreviations

IN: internode; PS: primary stems; TS: transitional stems; SS: secondary stems; DE-miRNA: differentially expressed miRNA; DEGs: differentially expressed genes; TFs: transcription factors; CTGs: candidate target genes; SCW: secondary cell wall; PCD: programmed cell death; FPKM: fragments per kilobase of gene per million; TPM: transcript per million; MFE: Minimum free energy; GO: gene ontology; KEGG: Kyoto Encyclopedia of Genes and Genomes; SE: standard error; sRNA: small RNA; BR: brassinosteroid; GA: gibberellin; miRNA: microRNA.

6 Declarations

6.1 Ethic approval and consent to participate

Not applicable.

6.2 Consent for publication

Not applicable.

6.3 Availability of data and materials

All data generated or analysed during this study are included in this published article and its supplementary information files.

6.4 Competing Interests

The authors declare that they have no competing interests.

6.5 Funding

The work was funded by the Fundamental Research Funds for the Central Non-profit Research Institution of CAF (CAFYBB2020ZA005, CAFYBB2018GB001), National Nature Science Fund of China (31770640), National Key Research and Development Project (2017YFC0504102).

6.6 Authors' Contributions

R. W. and M. R.: Finished most of experiment and measurements; S. T. and C. L.: participated in rising seeding of poplar; H. C.: participated in partly enrichment analysis; Y. L.: participated in genes expression pattern of poplar; H. Z. and M. S.: wrote manuscript; H. W.: performed data analysis and wrote manuscript; Z. W.: designed the experiments, performed data analysis, and wrote manuscript; All the authors read and approved the final version of the manuscript.

6.7 Acknowledgments

Not applicable.

7 References

1. Zhong R, Lee C, Ye ZH: **Functional characterization of poplar wood-associated NAC domain transcription factors**. *Plant Physiol* 2010, **152**(2):1044-1055.
2. Quan M, Liang X, Lu W, Xin L, Song F, Si J, Du Q, Zhang D: **Association Genetics in Populus Reveal the Allelic Interactions of Pto-MIR167a and Its Targets in Wood Formation**. *Frontiers in Plant Science* 2018, **9**:744-.
3. Zhong R, McCarthy RL, Lee C, Ye ZH: **Dissection of the transcriptional program regulating secondary wall biosynthesis during wood formation in poplar**. *Plant Physiol* 2011, **157**(3):1452-1468.
4. Takata N, Awano T, Nakata MT, Sano Y, Sakamoto S, Mitsuda N, Taniguchi T: **Populus NST/SND orthologs are key regulators of secondary cell wall formation in wood fibers, phloem fibers and xylem ray parenchyma cells**. *Tree Physiol* 2019, **39**(4):514-525.
5. Xu P, Kong Y, Song D, Huang C, Li X, Li L: **Conservation and functional influence of alternative splicing in wood formation of Populus and Eucalyptus**. *BMC Genomics* 2014, **15**:780.
6. Liu H, Yu W, Wu J, Li Z, Li H, Zhou J, Hu J, Lu Y: **Identification and characterization of circular RNAs during wood formation of poplars in acclimation to low nitrogen availability**. *Planta* 2020, **251**(2):47.
7. Quan M, Wang Q, Phangthavong S, Yang X, Song Y, Du Q, Zhang D: **Association Studies in Populus tomentosa Reveal the Genetic Interactions of Pto-MIR156c and Its Targets in Wood Formation**. *Front Plant Sci* 2016, **7**:1159.
8. Puzey JR, Karger A, Axtell M, Kramer EM: **Deep annotation of Populus trichocarpa microRNAs from diverse tissue sets**. *Plos One* 2012, **7**(3):e33034.

9. Yamamuro C, Zhu JK, Yang Z: **Epigenetic Modifications and Plant Hormone Action**. *Molecular plant* 2016, **9**(1):57-70.
10. Liu S, Mi X, Zhang R, An Y, Zhou Q, Yang T, Xia X, Guo R, Wang X, Wei C: **Integrated analysis of miRNAs and their targets reveals that miR319c/TCP2 regulates apical bud burst in tea plant (Camellia sinensis)**. *Planta* 2019, **250**(4):1111-1129.
11. Yang R, Li P, Mei H, Wang D, Sun J, Yang C, Hao L, Cao S, Chu C, Hu S *et al*: **Fine-Tuning of MiR528 Accumulation Modulates Flowering Time in Rice**. *Mol Plant* 2019, **12**(8):1103-1113.
12. Zhao Y, Lin S, Qiu Z, Cao D, Wen J, Deng X, Wang X, Lin J, Li X: **MicroRNA857 Is Involved in the Regulation of Secondary Growth of Vascular Tissues in Arabidopsis**. *Plant Physiology* 2015:pp.01011.02015.
13. Lu S, Li Q, Wei H, Chang MJ, Tunlaya-Anukit S, Kim H, Liu J, Song J, Sun YH, Yuan L *et al*: **Ptr-miR397a is a negative regulator of laccase genes affecting lignin content in Populus trichocarpa**. *Proc Natl Acad Sci U S A* 2013, **110**(26):10848-10853.
14. Chen B, Chen J, Du Q, Zhou D, Wang L, Xie J, Li Y, Zhang D: **Genetic variants in microRNA biogenesis genes as novel indicators for secondary growth in Populus**. *The New phytologist* 2018, **219**(4):1263-1282.
15. Chen B, Du Q, Chen J, Yang X, Tian J, Li B, Zhang D: **Dissection of allelic interactions among Pto-miR257 and its targets and their effects on growth and wood properties in Populus**. *Heredity* 2016, **117**(2):73-83.
16. Xiao L, Quan M, Du Q, Chen J, Xie J, Zhang D: **Allelic Interactions among Pto-MIR475b and Its Four Target Genes Potentially Affect Growth and Wood Properties in Populus**. *Front Plant Sci* 2017, **8**:1055.
17. Wang JW, Park MY, Wang LJ, Koo Y, Chen XY, Weigel D, Poethig RS: **miRNA control of vegetative phase change in trees**. *PLoS Genet* 2011, **7**(2):e1002012.
18. Du J, Miura E, Robischon M, Martinez C, Groover A: **The Populus Class III HD ZIP transcription factor POPCORONA affects cell differentiation during secondary growth of woody stems**. *PloS one* 2011, **6**(2):e17458.
19. Srivastava S, Zheng Y, Kudapa H, Jagadeeswaran G, Hivrale V, Varshney RK, Sunkar R: **High throughput sequencing of small RNA component of leaves and inflorescence revealed conserved and novel miRNAs as well as phasiRNA loci in chickpea**. *Plant Sci* 2015, **235**:46-57.
20. Brodersen P, Sakvarelidze-Achard L, Bruun-Rasmussen M, Dunoyer P, Yamamoto YY, Sieburth L, Voinnet O: **Widespread translational inhibition by plant miRNAs and siRNAs**. *Science* 2008, **320**(5880):1185-1190.
21. Rhoades MW, Reinhart BJ, Lim LP, Burge CB, Bartel B, Bartel DP: **Prediction of plant microRNA targets**. *Cell* 2002, **110**(4):513-520.
22. He CY, Cui K, Zhang JG, Duan AG, Zeng YF: **Next-generation sequencing-based mRNA and microRNA expression profiling analysis revealed pathways involved in the rapid growth of developing culms in Moso bamboo**. *BMC Plant Biol* 2013, **13**:119.

23. Pei H, Ma N, Chen J, Zheng Y, Tian J, Li J, Zhang S, Fei Z, Gao J: **Integrative analysis of miRNA and mRNA profiles in response to ethylene in rose petals during flower opening**. *Plos One* 2013, **8**(5):e64290.
24. Li J, Ding Q, Wang F, Zhang Y, Li H, Gao J: **Integrative Analysis of mRNA and miRNA Expression Profiles of the Tuberous Root Development at Seedling Stages in Turnips**. *Plos One* 2015, **10**(9):e0137983.
25. Prassinos C, Ko JH, Yang J, Han KH: **Transcriptome profiling of vertical stem segments provides insights into the genetic regulation of secondary growth in hybrid aspen trees**. *Plant Cell Physiol* 2005, **46**(8):1213-1225.
26. Dharmawardhana P, Brunner AM, Strauss SH: **Genome-wide transcriptome analysis of the transition from primary to secondary stem development in Populus trichocarpa**. *BMC Genomics* 2010, **11**:150.
27. Liu J, Hai G, Wang C, Cao S, Xu W, Jia Z, Yang C, Wang JP, Dai S, Cheng Y: **Comparative proteomic analysis of Populus trichocarpa early stem from primary to secondary growth**. *J Proteomics* 2015, **126**:94-108.
28. Zhang Y, Liu C, Cheng H, Tian S, Liu Y, Wang S, Zhang H, Saqib M, Wei H, Wei Z: **DNA methylation and its effects on gene expression during primary to secondary growth in poplar stems**. *BMC Genomics* 2020, **21**(1):498.
29. Zhang J, Xu Y, Huan Q, Chong K: **Deep sequencing of Brachypodium small RNAs at the global genome level identifies microRNAs involved in cold stress response**. *BMC Genomics* 2009, **10**:449.
30. Liu S, Hu Q, Sha L, Li Q, Yang X, Wang X, Wang S: **Expression of wild-type PtrIAA14.1, a poplar Aux/IAA gene causes morphological changes in Arabidopsis**. 2015.
31. Gao R, Wang Y, Gruber MY, Hannoufa A: **miR156/SPL10 Modulates Lateral Root Development, Branching and Leaf Morphology in Arabidopsis by Silencing AGAMOUS-LIKE 79**. *Front Plant Sci* 2017, **8**:2226.
32. Shikata M, Koyama T, Mitsuda N, Ohme-Takagi M: **Arabidopsis SBP-box genes SPL10, SPL11 and SPL2 control morphological change in association with shoot maturation in the reproductive phase**. *Plant Cell Physiol* 2009, **50**(12):2133-2145.
33. Usami T, Horiguchi G, Yano S, Tsukaya H: **The more and smaller cells mutants of Arabidopsis thaliana identify novel roles for SQUAMOSA PROMOTER BINDING PROTEIN-LIKE genes in the control of heteroblasty**. *Development* 2009, **136**(6):955-964.
34. Preston JC, Hileman LC: **Functional Evolution in the Plant SQUAMOSA-PROMOTER BINDING PROTEIN-LIKE (SPL) Gene Family**. *Front Plant Sci* 2013, **4**:80.
35. Huijser P, Schmid M: **The control of developmental phase transitions in plants**. *Development* 2011, **138**(19):4117-4129.
36. Xue T, Liu ZH, Dai XH, Xiang FN: **Primary root growth in Arabidopsis thaliana is inhibited by the miR159 mediated repression of MYB33, MYB65 and MYB101**. *Plant Sci* 2017, **262**:182-189.
37. Bechtold U, Penfold CA, Jenkins DJ, Legaie R, Moore JD, Lawson T, Matthews JSA, Vialet-Chabrand SRM, Baxter L, Subramaniam S *et al*: **Time-Series Transcriptomics Reveals That AGAMOUS-LIKE22**

Affects Primary Metabolism and Developmental Processes in Drought-Stressed Arabidopsis. *Plant Cell* 2016, **28**(2):345-366.

38. Ikeda M, Fujiwara S, Mitsuda N, Ohme-Takagi M: **A triantagonistic basic helix-loop-helix system regulates cell elongation in Arabidopsis**. *Plant Cell* 2012, **24**(11):4483-4497.
39. Zhong R, Lee C, Zhou J, McCarthy RL, Ye ZH: **A battery of transcription factors involved in the regulation of secondary cell wall biosynthesis in Arabidopsis**. *Plant Cell* 2008, **20**(10):2763-2782.
40. Zhou J, Lee C, Zhong R, Ye ZH: **MYB58 and MYB63 are transcriptional activators of the lignin biosynthetic pathway during secondary cell wall formation in Arabidopsis**. *Plant Cell* 2009, **21**(1):248-266.
41. Tsugama D, Matsuyama K, Ide M, Hayashi M, Fujino K, Masuda K: **A putative MYB35 ortholog is a candidate for the sex-determining genes in Asparagus officinalis**. *Sci Rep-Uk* 2017, **7**.
42. Li SF, Allen PJ, Napoli RS, Browne RG, Pham H, Parish RW: **MYB-bHLH-TTG1 Regulates Arabidopsis Seed Coat Biosynthesis Pathways Directly and Indirectly via Multiple Tiers of Transcription Factors**. *Plant and Cell Physiology* 2020, **61**(5):1005-1018.
43. Liu CG, Jun JH, Dixon RA: **MYB5 and MYB14 Play Pivotal Roles in Seed Coat Polymer Biosynthesis in Medicago truncatula**. *Plant Physiol* 2014, **165**(4):1424-1439.
44. Dixon RA, Barros J: **Lignin biosynthesis: old roads revisited and new roads explored**. *Open Biol* 2019, **9**(12).
45. Liu Y, Wei M, Hou C, Lu T, Liu L, Wei H, Cheng Y, Wei Z: **Functional Characterization of Populus PsnSHN2 in Coordinated Regulation of Secondary Wall Components in Tobacco**. *Sci Rep* 2017, **7**(1):42.
46. Ko JH, Jeon HW, Kim WC, Kim JY, Han KH: **The MYB46/MYB83-mediated transcriptional regulatory programme is a gatekeeper of secondary wall biosynthesis**. *Ann Bot* 2014, **114**(6):1099-1107.
47. Ko JH, Kim WC, Han KH: **Ectopic expression of MYB46 identifies transcriptional regulatory genes involved in secondary wall biosynthesis in Arabidopsis**. *Plant J* 2009, **60**(4):649-665.
48. Xun Q, Wu Y, Li H, Chang J, Ou Y, He K, Gou X, Tax FE, Li J: **Two receptor-like protein kinases, MUSTACHES and MUSTACHES-LIKE, regulate lateral root development in Arabidopsis thaliana**. *New Phytol* 2020, **227**(4):1157-1173.
49. Kim J, Jung JH, Reyes JL, Kim YS, Kim SY, Chung KS, Kim JA, Lee M, Lee Y, Narry Kim V *et al*: **microRNA-directed cleavage of ATHB15 mRNA regulates vascular development in Arabidopsis inflorescence stems**. *Plant J* 2005, **42**(1):84-94.
50. Baima S, Possenti M, Matteucci A, Wisman E, Altamura MM, Ruberti I, Morelli G: **The arabidopsis ATHB-8 HD-zip protein acts as a differentiation-promoting transcription factor of the vascular meristems**. *Plant Physiol* 2001, **126**(2):643-655.
51. Münevver, Doramac, Michael, Foley, David, Horvath, Alvaro: **Glyphosate's impact on vegetative growth in leafy spurge identifies molecular processes and hormone cross-talk associated with increased branching**. *Bmc Genomics* 2015.

52. Belén PM, Jesús MRJ, Cánovas FM, Fernando G: **Overexpression of a cytosolic NADP+-isocitrate dehydrogenase causes alterations in the vascular development of hybrid poplars**. *Tree Physiology* 2018(7):7.
53. Deyoung BJ, Bickle KL, Schrage KJ, Muskett P, Patel K, Clark SE: **The CLAVATA1-related BAM1, BAM2 and BAM3 receptor kinase-like proteins are required for meristem function in Arabidopsis**. *Plant Journal* 2006, **45**(1):1-16.
54. Masubelele NH, Dewitte W, Menges M, Maughan S, Collins C, Huntley R, Nieuwland J, Scofield S, Murray JA: **D-type cyclins activate division in the root apex to promote seed germination in Arabidopsis**. *Proc Natl Acad Sci U S A* 2005, **102**(43):15694-15699.
55. Vogel JP, Raab TK, Somerville CR, Somerville SC: **Mutations in PMR5 result in powdery mildew resistance and altered cell wall composition**. *Plant J* 2004, **40**(6):968-978.
56. Laffont C, Blanchet S, Lapierre C, Brocard L, Ratet P, Crespi M, Mathesius U, Frugier F: **The compact root architecture1 gene regulates lignification, flavonoid production, and polar auxin transport in Medicago truncatula**. *Plant Physiol* 2010, **153**(4):1597-1607.
57. Cruz-Valderrama JE, Gomez-Maqueo X, Salazar-Iribe A, Zuniga-Sanchez E, Hernandez-Barrera A, Quezada-Rodriguez E, Gamboa-deBuen A: **Overview of the Role of Cell Wall DUF642 Proteins in Plant Development**. *Int J Mol Sci* 2019, **20**(13).
58. O'Malley DM, Whetten R, Bao W, Chen CL, Sederoff RR: **The role of of laccase in lignification**. *Plant Journal* 2010, **4**(5):751-757.
59. Robert, Sykes, Erica, Gjersing, Kirk, Foutz, William: **Down-regulation of p-coumaroyl quinate/shikimate 3'-hydroxylase (C3'H) and cinnamate 4-hydroxylase (C4H) genes in the lignin biosynthetic pathway of Eucalyptus urophylla?×?E. grandis leads to improved sugar release**. *Biotechnology for Biofuels* 2015.
60. Zhao Q, Nakashima J, Chen F, Yin Y, Fu C, Yun J, Shao H, Wang X, Wang ZY, Dixon RA: **Laccase is necessary and nonredundant with peroxidase for lignin polymerization during vascular development in Arabidopsis**. *Plant Cell* 2013, **25**(10):3976-3987.
61. Wang HY, Wang J, Gao P, Jiao GL, Zhao PM, Li Y, Wang GL, Xia GX: **Down-regulation of GhADF1 gene expression affects cotton fibre properties**. *Plant Biotechnol J* 2009, **7**(1):13-23.
62. Aoyagi S, Sugiyama M, Fukuda H: **BEN1 and ZEN1 cDNAs encoding S1-type DNases that are associated with programmed cell death in plants1**. *FEBS Letters* 1998, **429**.
63. Huang X, Liu X, Chen X, Snyder A, Song WY: **Members of the XB3 Family from Diverse Plant Species Induce Programmed Cell Death in Nicotiana benthamiana**. *PloS one* 2013, **8**(5):e63868.
64. Bouwmeester, Klaas, Cordewener, Jan, H., G., America, Antoine, H., P.: **Arabidopsis Lectin Receptor Kinases LecRK-IX.1 and LecRK-IX.2 Are Functional Analogs in Regulating Phytophthora Resistance and Plant Cell Death**. *Molecular Plant Microbe Interactions* 2015.
65. Knoth, Colleen, Ringler, Jon, Dangl, Jeffery, L., Eulgem, Thomas: **Arabidopsis WRKY70 Is Required for Full RPP4 -Mediated Disease Resistance and Basal Defense Against Hyaloperonospora parasitica**. *Mpmi* 2007.

66. Niinemets ü, Lukjanova A: **Total Foliar Area and Average Leaf Age May Be More Strongly Associated with Branching Frequency Than with Leaf Longevity in Temperate Conifers**. *New Phytologist* 2003, **158**(1):75-89.
67. Evers JB, Vos J, Andrieu B, STRUIK aPC: **Cessation of Tillering in Spring Wheat in Relation to Light Interception and Red : Far-red Ratio**. *Annals of Botany* 2006, **97**(4):649-658.
68. Kawamura K, Takeda H: **Rules of crown development in the clonal shrub\\r Vaccinium hirtum\\r in a low-light understory: a quantitative analysis of architecture**. *Canadian Journal of Botany* 2004, **82**(3):329-339.
69. Takahashi H, Imamura T, Konno N, Takeda T, Fujita K, Konishi T, Nishihara M, Uchimiya H: **The gentio-oligosaccharide gentiobiose functions in the modulation of bud dormancy in the herbaceous perennial Gentiana**. *Plant Cell* 2014, **26**(10):3949-3963.
70. Tamaki H, Konishi M, Daimon Y, Aida M, Tasaka M, Sugiyama M: **Identification of novel meristem factors involved in shoot regeneration through the analysis of temperature-sensitive mutants of Arabidopsis**. *Plant Journal* 2009, **57**(6):1027-1039.
71. Limin AE, Fowler DB: **Low-temperature tolerance and genetic potential in wheat (Triticum aestivumL.): response to photoperiod, vernalization, and plant development**. *Planta* 2006, **224**(2):360-366.
72. Hall AJ, Catley JL, Walton EF: **The effect of forcing temperature on peony shoot and flower development**. *Scientia Horticulturae* 2007, **113**(2):0-195.
73. Liu Y, Ou Y, Sun L, Li W, Yang J, Zhang X, Hu Y: **Alcohol dehydrogenase of Candida albicans triggers differentiation of THP-1 cells into macrophages**. *J Adv Res* 2019, **18**:137-145.
74. Zhu L, Ni W, Liu S, Cai B, Xing H, Wang S: **Transcriptomics Analysis of Apple Leaves in Response to Alternaria alternata Apple Pathotype Infection**. *Front Plant Sci* 2017, **8**:22.
75. Velasquez SM, Ricardi MM, Poulsen CP, Oikawa A, Dilokpimol A, Halim A, Mangano S, Denita Juarez SP, Marzol E, Salgado Salter JD *et al*: **Complex regulation of prolyl-4-hydroxylases impacts root hair expansion**. *Molecular plant* 2015, **8**(5):734-746.
76. Barman S, Ghosh R, Sengupta S, Mandal NC: **Longterm storage of post-packaged bread by controlling spoilage pathogens using Lactobacillus fermentum C14 isolated from homemade curd**. *PloS one* 2017, **12**(8):e0184020.
77. Heisler MG, Hamant O, Krupinski P, Uyttewaal M, Ohno C, Jonsson H, Traas J, Meyerowitz EM: **Alignment between PIN1 polarity and microtubule orientation in the shoot apical meristem reveals a tight coupling between morphogenesis and auxin transport**. *PLoS Biol* 2010, **8**(10):e1000516.
78. Rinaldi R, Jastrzebski R, Clough MT, Ralph J, Kennema M, Bruijnincx PC, Weckhuysen BM: **Paving the Way for Lignin Valorisation: Recent Advances in Bioengineering, Biorefining and Catalysis**. *Angewandte Chemie (International ed in English)* 2016, **55**(29):8164-8215.
79. Xie M, Muchero W, Bryan AC, Yee K, Guo HB, Zhang J, Tschaplinski TJ, Singan VR, Lindquist E, Payyavula RS *et al*: **A 5-Enolpyruvylshikimate 3-Phosphate Synthase Functions as a Transcriptional Repressor in Populus**. *Plant Cell* 2018, **30**(7):1645-1660.

80. Roeschlin RA, Favaro MA, Chiesa MA, Alemano S, Vojnov AA, Castagnaro AP, Filippone MP, Gmitter FG, Jr., Gadea J, Marano MR: **Resistance to citrus canker induced by a variant of Xanthomonas citri ssp. citri is associated with a hypersensitive cell death response involving autophagy-associated vacuolar processes**. *Molecular plant pathology* 2017, **18**(9):1267-1281.
81. Kevin, Vidot, Cédric, Gaillard, Camille, Rivard, René, Siret, Marc, Lahaye: **Cryo-laser scanning confocal microscopy of diffusible plant compounds**. *Plant Methods* 2018.
82. Preeti J, Basanti M, Zahoor KM, Savita L, Archana S, Nandicoori VK: **Delineating FtsQ mediated regulation of cell division in Mycobacterium tuberculosis**. *Journal of Biological Chemistry* 2018:jbc.RA118.003628-.
83. Geng P, Zhang S, Liu J, Zhao C, Wu J, Cao Y, Fu C, Han X, He H, Zhao Q: **MYB20, MYB42, MYB43, and MYB85 Regulate Phenylalanine and Lignin Biosynthesis during Secondary Cell Wall Formation**. *Plant Physiol* 2020, **182**(3):1272-1283.
84. Barakat A, Wall PK, Diloreto S, Depamphilis CW, Carlson JE: **Conservation and divergence of microRNAs in Populus**. *BMC Genomics* 2007, **8**:481.
85. Wan LC, Wang F, Guo X, Lu S, Qiu Z, Zhao Y, Zhang H, Lin J: **Identification and characterization of small non-coding RNAs from Chinese fir by high throughput sequencing**. *BMC Plant Biol* 2012, **12**:146.
86. Wang C, Shangguan L, Kibet KN, Wang X, Han J, Song C, Fang J: **Characterization of microRNAs identified in a table grapevine cultivar with validation of computationally predicted grapevine miRNAs by miR-RACE**. *Plos One* 2011, **6**(7):e21259.
87. Xie F, Wang Q, Zhang B: **Global microRNA modification in cotton (Gossypium hirsutum L.)**. *Plant Biotechnol J* 2015, **13**(4):492-500.
88. Ren Y, Chen L, Zhang Y, Kang X, Zhang Z, Wang Y: **Identification and characterization of salt-responsive microRNAs in Populus tomentosa by high-throughput sequencing**. *Biochimie* 2013, **95**(4):743-750.
89. Yakovlev IA, Fossdal CG, Johnsen y: **MicroRNAs, the epigenetic memory and climatic adaptation in Norway spruce**. *New Phytologist*, **187**(4):1154-1169.
90. Wei X, Jin X, Ndayambaza B, Min X, Zhang Z, Wang Y, Liu W: **Transcriptome-Wide Characterization and Functional Identification of the Aquaporin Gene Family During Drought Stress in Common Vetch**. *DNA Cell Biol* 2019, **38**(4):374-384.
91. Peragine A, Yoshikawa M, Wu G, Albrecht HL, Poethig RS: **SGS3 and SGS2/SDE1/RDR6 are required for juvenile development and the production of trans-acting siRNAs in Arabidopsis**. *Genes Dev* 2004, **18**(19):2368-2379.
92. Dolgosheina EV MR, Aksay G, Sahinalp SC, Magrini V, Mardis, ER MJ, Unrau PJ.: **Conifers have a unique small RNA silencing signature.** *RNA* 2008, **14**:1508-1515.
93. Addo-Quaye C, Eshoo TW, Bartel DP, Axtell MJ: **Endogenous siRNA and miRNA targets identified by sequencing of the Arabidopsis degradome**. *Curr Biol* 2008, **18**(10):758-762.

94. Zhang M, Dong Y, Nie L, Lu M, Fu C, Yu L: **High-throughput sequencing reveals miRNA effects on the primary and secondary production properties in long-term subcultured Taxus cells**. *Front Plant Sci* 2015, **6**:604.
95. Lopez-Gomollon S, Mohorianu I, Szittya G, Moulton V, Dalmay T: **Diverse correlation patterns between microRNAs and their targets during tomato fruit development indicates different modes of microRNA actions**. *Planta* 2012, **236**(6):1875-1887.
96. Nikovics K, Blein T, Peaucelle A, Ishida T, Morin H, Aida M, Laufs P: **The balance between the MIR164A and CUC2 genes controls leaf margin serration in Arabidopsis**. *Plant Cell* 2006, **18**(11):2929-2945.
97. Donaire L, Pedrola L, Rosa Rde L, Llave C: **High-throughput sequencing of RNA silencing-associated small RNAs in olive (Olea europaea L.)**. *Plos One* 2011, **6**(11):e27916.
98. Qiu Z, Li X, Zhao Y, Zhang M, Wan Y, Cao D, Lu S, Lin J: **Genome-wide analysis reveals dynamic changes in expression of microRNAs during vascular cambium development in Chinese fir, Cunninghamia lanceolata**. *J Exp Bot* 2015, **66**(11):3041-3054.
99. Wu G, Park MY, Conway SR, Wang JW, Weigel D, Poethig RS: **The sequential action of miR156 and miR172 regulates developmental timing in Arabidopsis**. *Cell* 2009, **138**(4):750-759.
100. Zhang L, Chia JM, Kumari S, Stein JC, Liu Z, Narechania A, Maher CA, Guill K, McMullen MD, Ware D: **A genome-wide characterization of microRNA genes in maize**. *PLoS Genet* 2009, **5**(11):e1000716.
101. Yu N, Niu QW, Ng KH, Chua NH: **The role of miR156/SPLs modules in Arabidopsis lateral root development**. *Plant J* 2015, **83**(4):673-685.
102. Jung JH, Seo YH, Seo PJ, Reyes JL, Yun J, Chua NH, Park CM: **The GIGANTEA-regulated microRNA172 mediates photoperiodic flowering independent of CONSTANS in Arabidopsis**. *Plant Cell* 2007, **19**(9):2736-2748.
103. Guo C, Xu Y, Shi M, Lai Y, Wu X, Wang H, Zhu Z, Poethig RS, Wu G: **Repression of miR156 by miR159 Regulates the Timing of the Juvenile-to-Adult Transition in Arabidopsis**. *Plant Cell* 2017, **29**(6):1293-1304.
104. Liebsch D, Palatnik JF: **MicroRNA miR396, GRF transcription factors and GIF co-regulators: a conserved plant growth regulatory module with potential for breeding and biotechnology**. *Curr Opin Plant Biol* 2020, **53**:31-42.
105. Wang L, Liu Z, Qiao M, Xiang F: **miR393 inhibits in vitro shoot regeneration in Arabidopsis thaliana via repressing TIR1**. *Plant Sci* 2018, **266**:1-8.
106. Li C, Lu S: **Genome-wide characterization and comparative analysis of R2R3-MYB transcription factors shows the complexity of MYB-associated regulatory networks in Salvia miltiorrhiza**. *BMC Genomics* 2014, **15**:277.
107. Li Y, Cui W, Qi X, Lin M, Qiao C, Zhong Y, Hu C, Fang J: **MicroRNA858 negatively regulates anthocyanin biosynthesis by repressing AaMYBC1 expression in kiwifruit (Actinidia arguta)**. *Plant Sci* 2020, **296**:110476.

108. Jia X, Shen J, Liu H, Li F, Ding N, Gao C, Pattanaik S, Patra B, Li R, Yuan L: **Small tandem target mimic-mediated blockage of microRNA858 induces anthocyanin accumulation in tomato**. *Planta* 2015, **242**(1):283-293.

109. Tirumalai V, Swetha C, Nair A, Pandit A, Shivaprasad PV: **miR828 and miR858 regulate VvMYB114 to promote anthocyanin and flavonol accumulation in grapes**. *J Exp Bot* 2019, **70**(18):4775-4792.

110. Guan X, Pang M, Nah G, Shi X, Ye W, Stelly DM, Chen ZJ: **miR828 and miR858 regulate homoeologous MYB2 gene functions in Arabidopsis trichome and cotton fibre development**. *Nat Commun* 2014, **5**:3050.

111. Piya S, Kihm C, Rice JH, Baum TJ, Hewezi T: **Cooperative Regulatory Functions of miR858 and MYB83 during Cyst Nematode Parasitism**. *Plant Physiol* 2017, **174**(3):1897-1912.

112. Ong SS, Wickneswari R: **Characterization of microRNAs expressed during secondary wall biosynthesis in Acacia mangium**. *Plos One* 2012, **7**(11):e49662.

113. DeYoung BJ, Bickle KL, Schrage KJ, Muskett P, Patel K, Clark SE: **The CLAVATA1-related BAM1, BAM2 and BAM3 receptor kinase-like proteins are required for meristem function in Arabidopsis**. *Plant J* 2006, **45**(1):1-16.

114. Pascual MB, Molina-Rueda JJ, Canovas FM, Gallardo F: **Overexpression of a cytosolic NADP+-isocitrate dehydrogenase causes alterations in the vascular development of hybrid poplars**. *Tree Physiol* 2018, **38**(7):992-1005.

115. Ceserani T, Trofka A, Gandotra N, Nelson T: **VH1/BRL2 receptor-like kinase interacts with vascular-specific adaptor proteins VIT and VIK to influence leaf venation**. *Plant J* 2009, **57**(6):1000-1014.

116. Sykes RW, Gjersing EL, Foutz K, Rottmann WH, Kuhn SA, Foster CE, Ziebell A, Turner GB, Decker SR, Hinchee MA *et al*: **Down-regulation of p-coumaroyl quinate/shikimate 3'-hydroxylase (C3'H) and cinnamate 4-hydroxylase (C4H) genes in the lignin biosynthetic pathway of Eucalyptus urophylla x E. grandis leads to improved sugar release**. *Biotechnol Biofuels* 2015, **8**:128.

117. Li S, Zhen C, Xu W, Wang C, Cheng Y: **Simple, rapid and efficient transformation of genotype Nisqually-1: a basic tool for the first sequenced model tree**. *Sci Rep* 2017, **7**(1):2638.

118. Friedlander MR, Mackowiak SD, Li N, Chen W, Rajewsky N: **miRDeep2 accurately identifies known and hundreds of novel microRNA genes in seven animal clades**. *Nucleic Acids Res* 2012, **40**(1):37-52.

119. Chen C, Ridzon DA, Broomer AJ, Zhou Z, Lee DH, Nguyen JT, Barbisin M, Xu NL, Mahuvakar VR, Andersen MR *et al*: **Real-time quantification of microRNAs by stem-loop RT-PCR**. *Nucleic Acids Res* 2005, **33**(20):e179.

120. Livak KJ, Schmittgen TD: **Analysis of relative gene expression data using real-time quantitative PCR and the 2(-Delta Delta C(T)) Method**. *Methods* 2001, **25**(4):402-408.

Figures

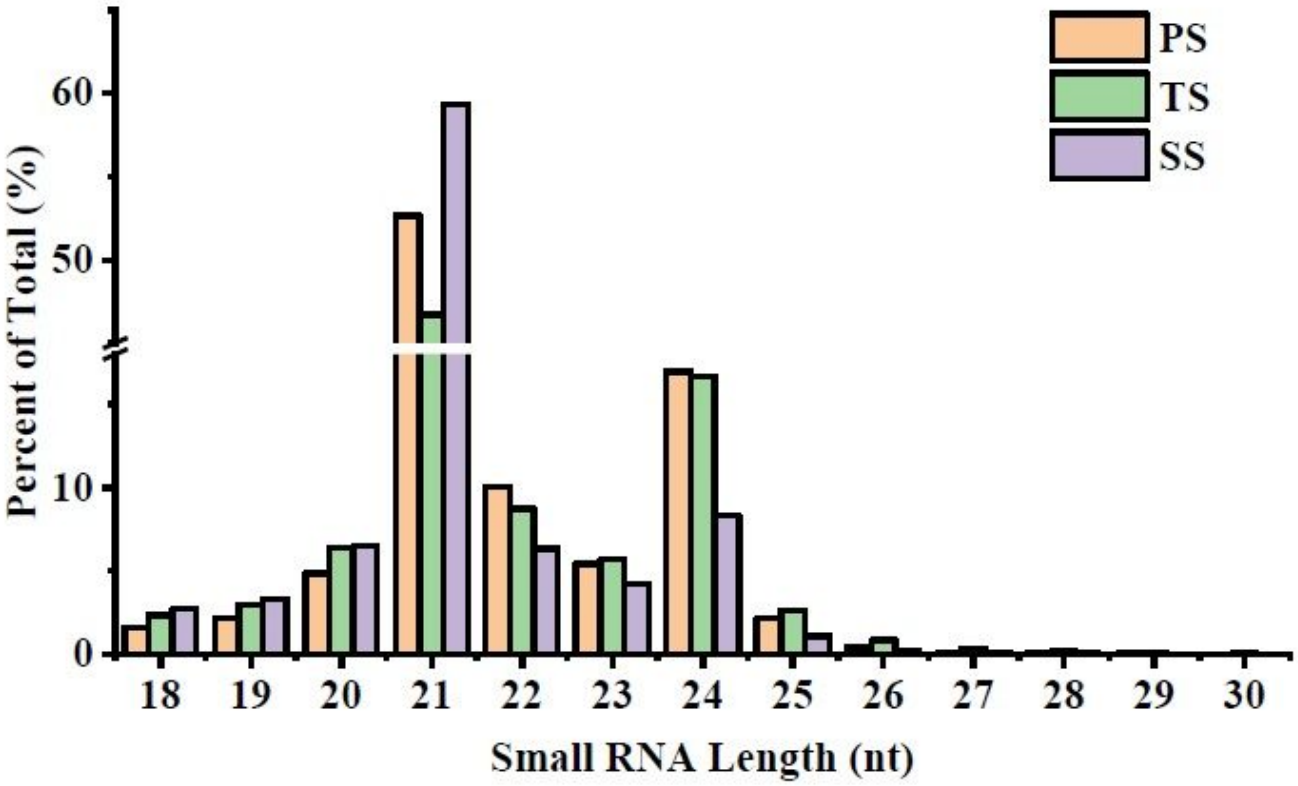

Figure 1

Length distribution of 18-30 nt small RNAs in PS, TS, and SS libraries. The x axis represents different lengths of sRNA, and the y axis represents percentage of sRNA in total. PS, TS and SS represent primary stage, transition stage, and secondary stage of stem of Populus trichocarpa, respectively.

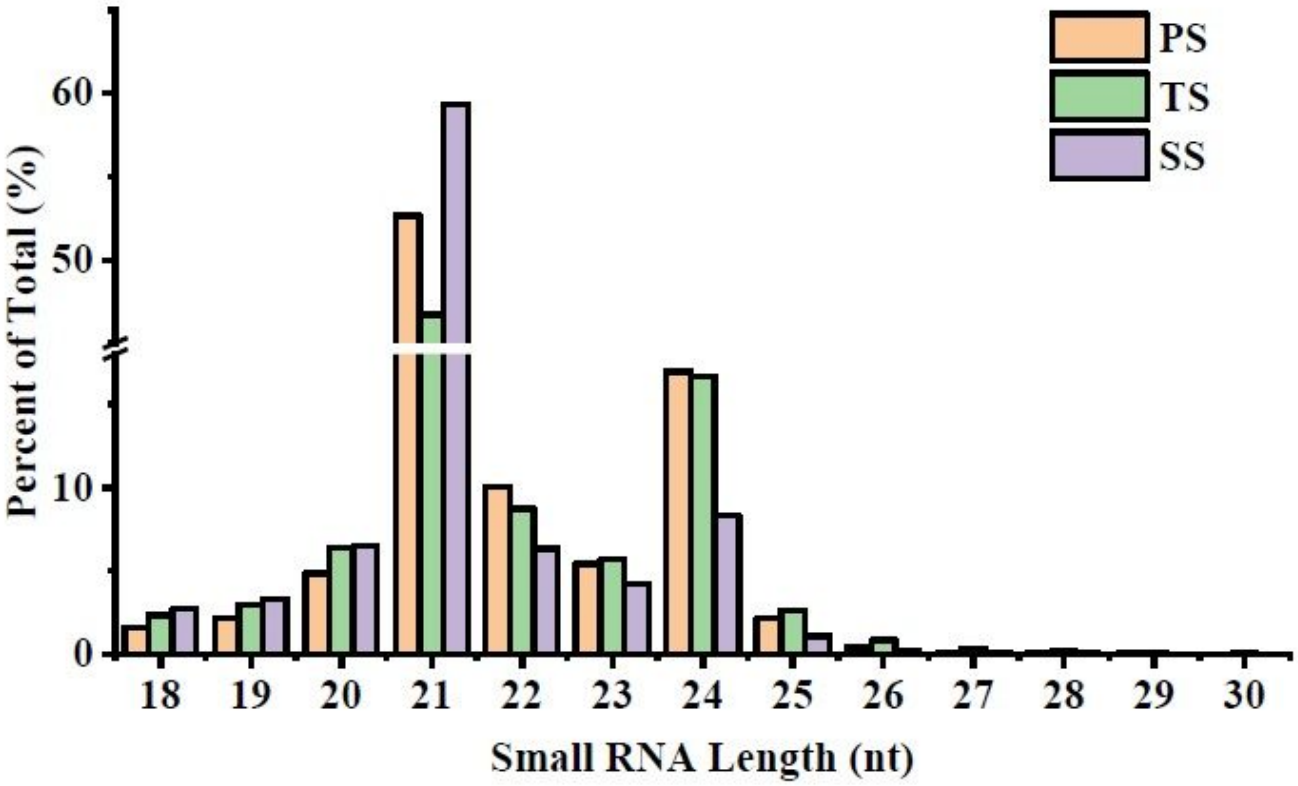

Figure 1

Length distribution of 18-30 nt small RNAs in PS, TS, and SS libraries. The x axis represents different lengths of sRNA, and the y axis represents percentage of sRNA in total. PS, TS and SS represent primary stage, transition stage, and secondary stage of stem of Populus trichocarpa, respectively.

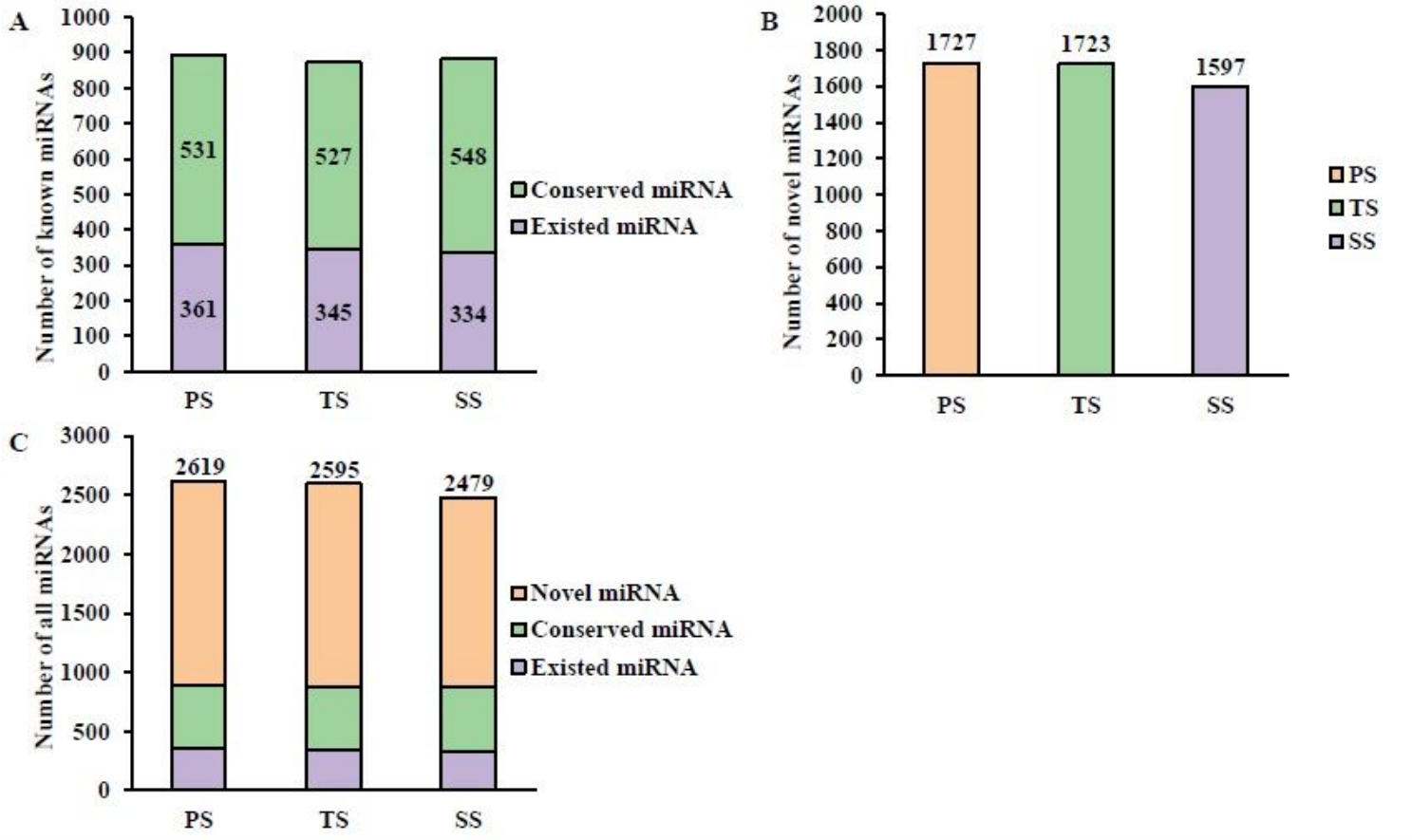

Figure 2

The number of different miRNAs in PS, TS, and SS of poplar. (A) The number of Known miRNAs (include Conserved miRNA and Existing miRNA) miRNA in different development stage. (B) The number of novel miRNAs in different development stage. (C) All identified miRNAs in different development stage.

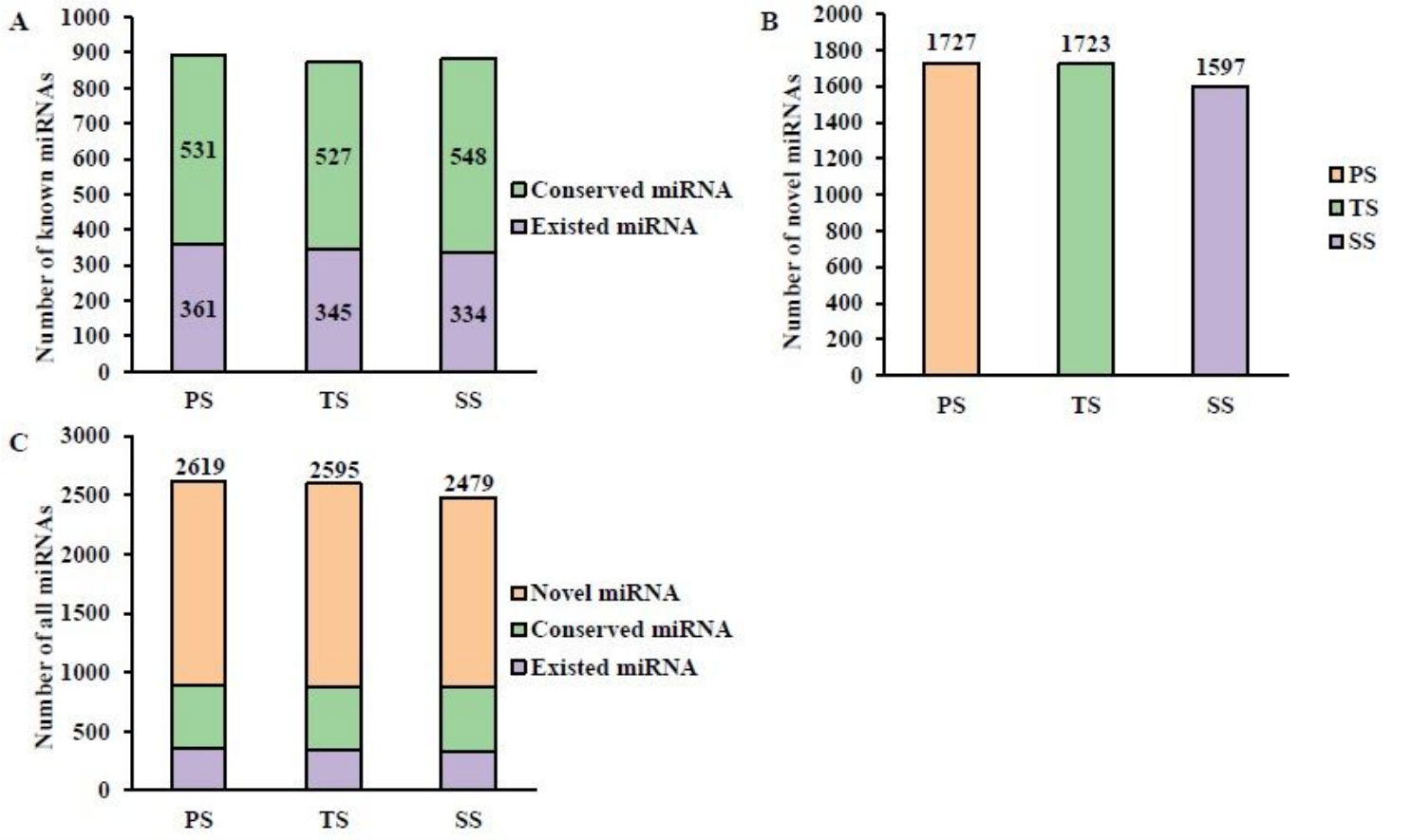

Figure 2

The number of different miRNAs in PS, TS, and SS of poplar. (A) The number of Known miRNAs (include Conserved miRNA and Existing miRNA) miRNA in different development stage. (B) The number of novel miRNAs in different development stage. (C) All identified miRNAs in different development stage.

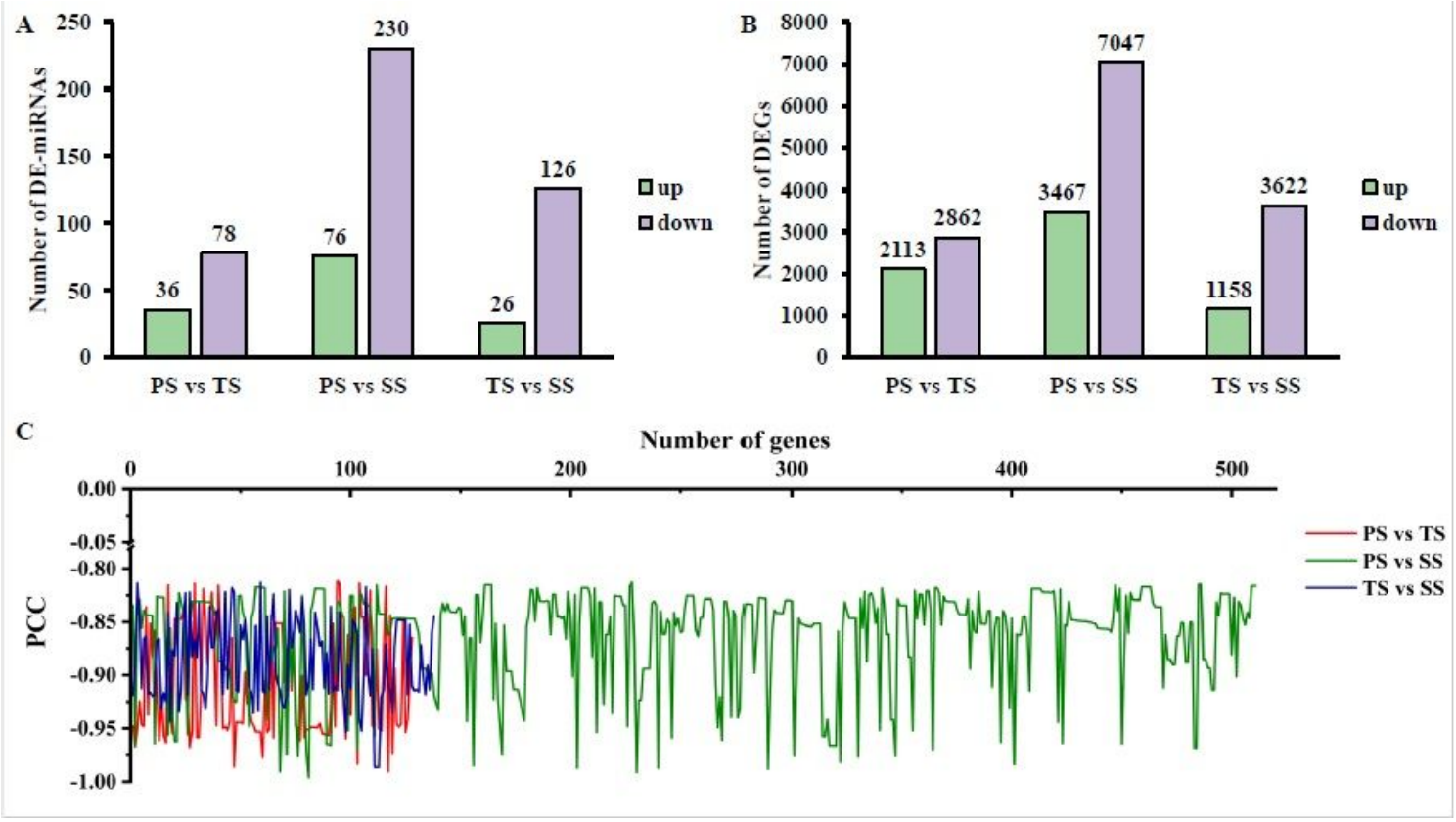

Figure 3

Significant small RNA and gene pairs in three developmental stages of poplar stems. (A) differentially expressed (DE)-miRNA quantity statistics. (B) Differentially expressed gene (DEG) quantity statistics. (C) Distribution of significant negative correlations of miRNA-target pairs. The x axis of (c) represents the number of miRNA-target pairs, and the y axis represents the Pearson correlation coefficients (PCCs). PS, TS and SS represent primary stage, transition stage, and secondary stage of stem of poplar, respectively.

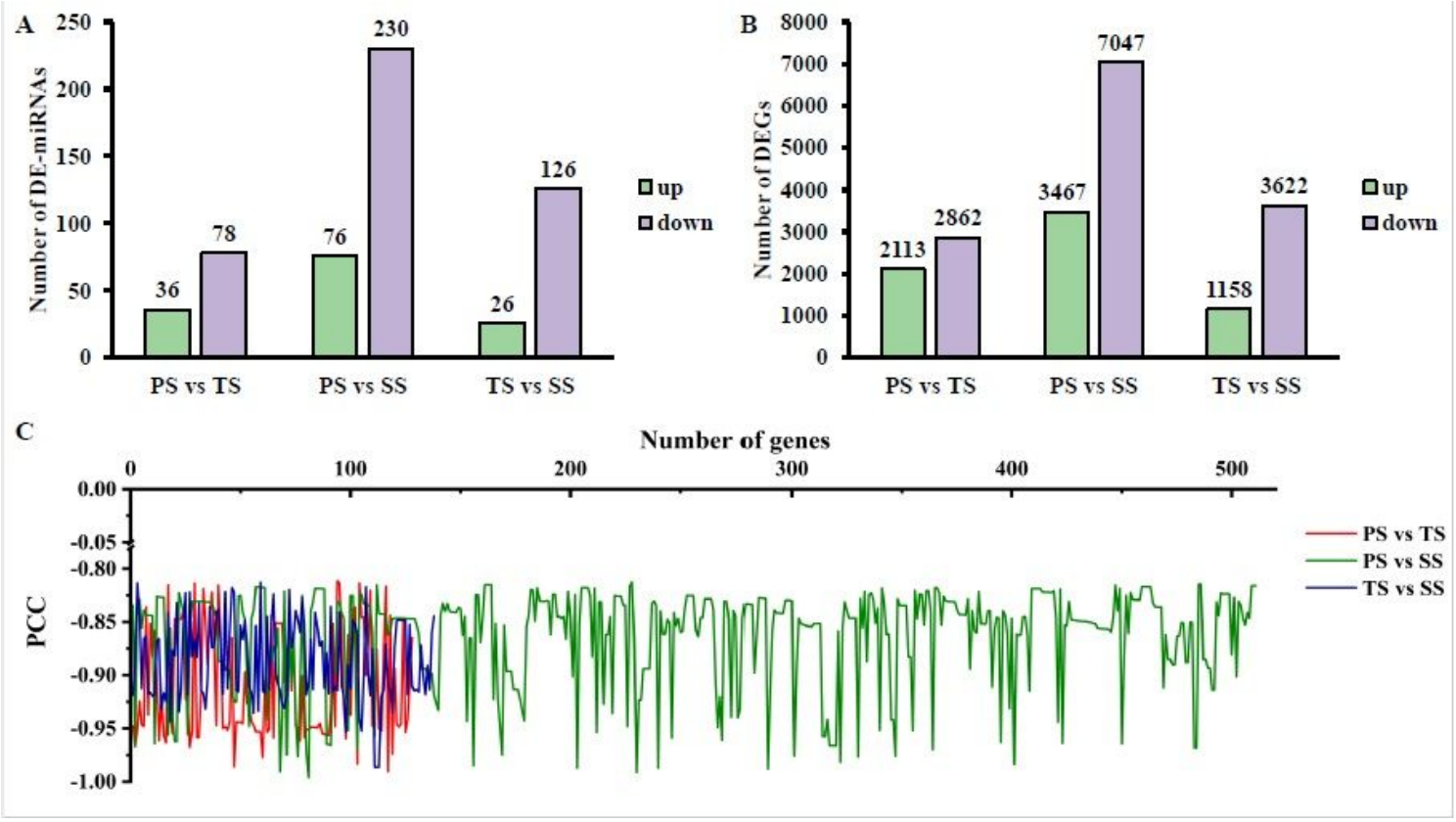

Figure 3

Significant small RNA and gene pairs in three developmental stages of poplar stems. (A) differentially expressed (DE)-miRNA quantity statistics. (B) Differentially expressed gene (DEG) quantity statistics. (C) Distribution of significant negative correlations of miRNA-target pairs. The x axis of (c) represents the number of miRNA-target pairs, and the y axis represents the Pearson correlation coefficients (PCCs). PS, TS and SS represent primary stage, transition stage, and secondary stage of stem of poplar, respectively.

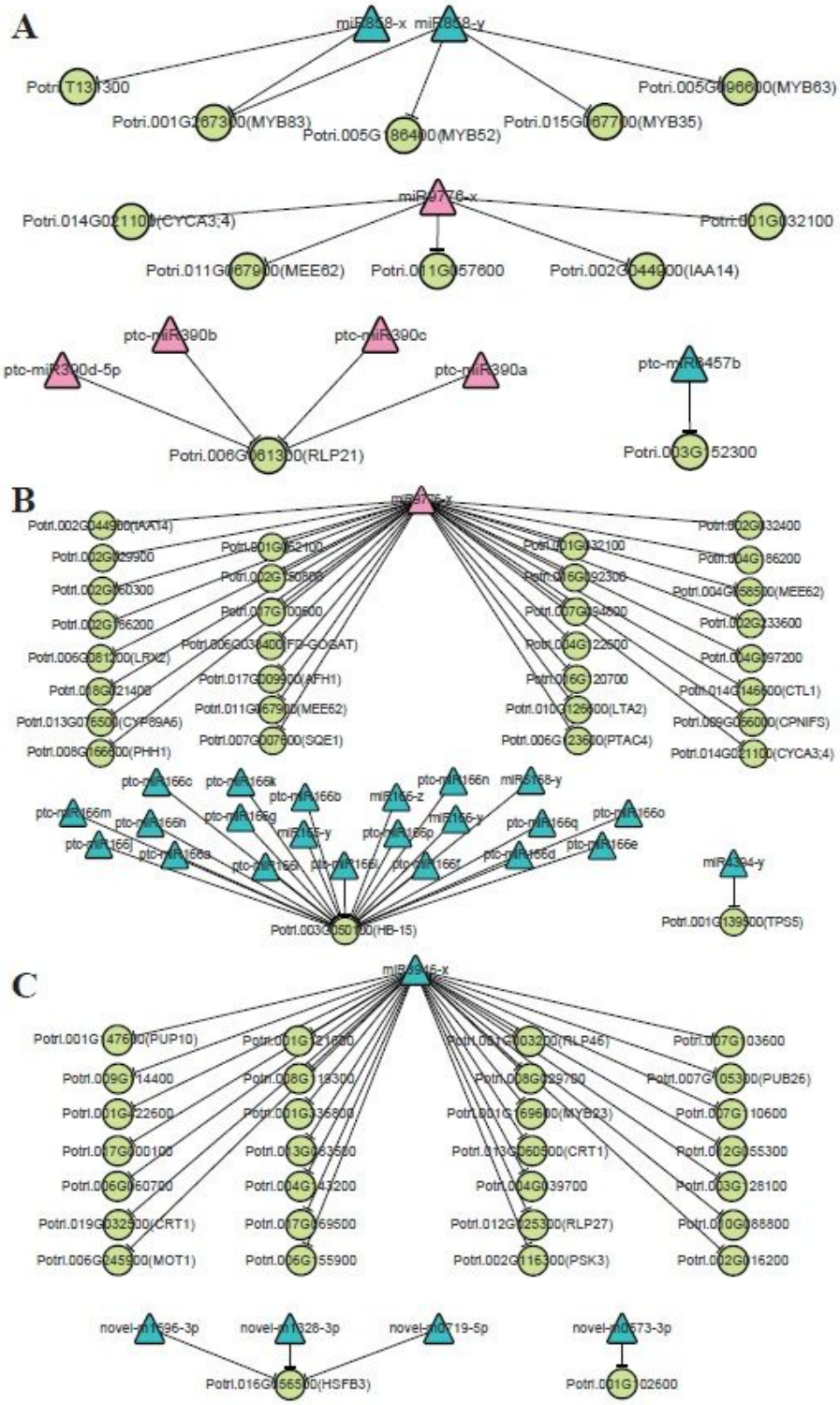

Figure 4

The regulatory relationships of DE-miRNAs and CTGs. (A) The regulatory relationships of DE-miRNAs and CTGs in PS vs TS. (B) The regulatory relationships of DE-miRNAs and CTGs in PS vs SS. (C) The regulatory relationships of DE-miRNAs and CTGs in TS vs SS. Pink represents up-regulated miRNA, Blue represents down-regulated miRNA, Green represents CTGs.

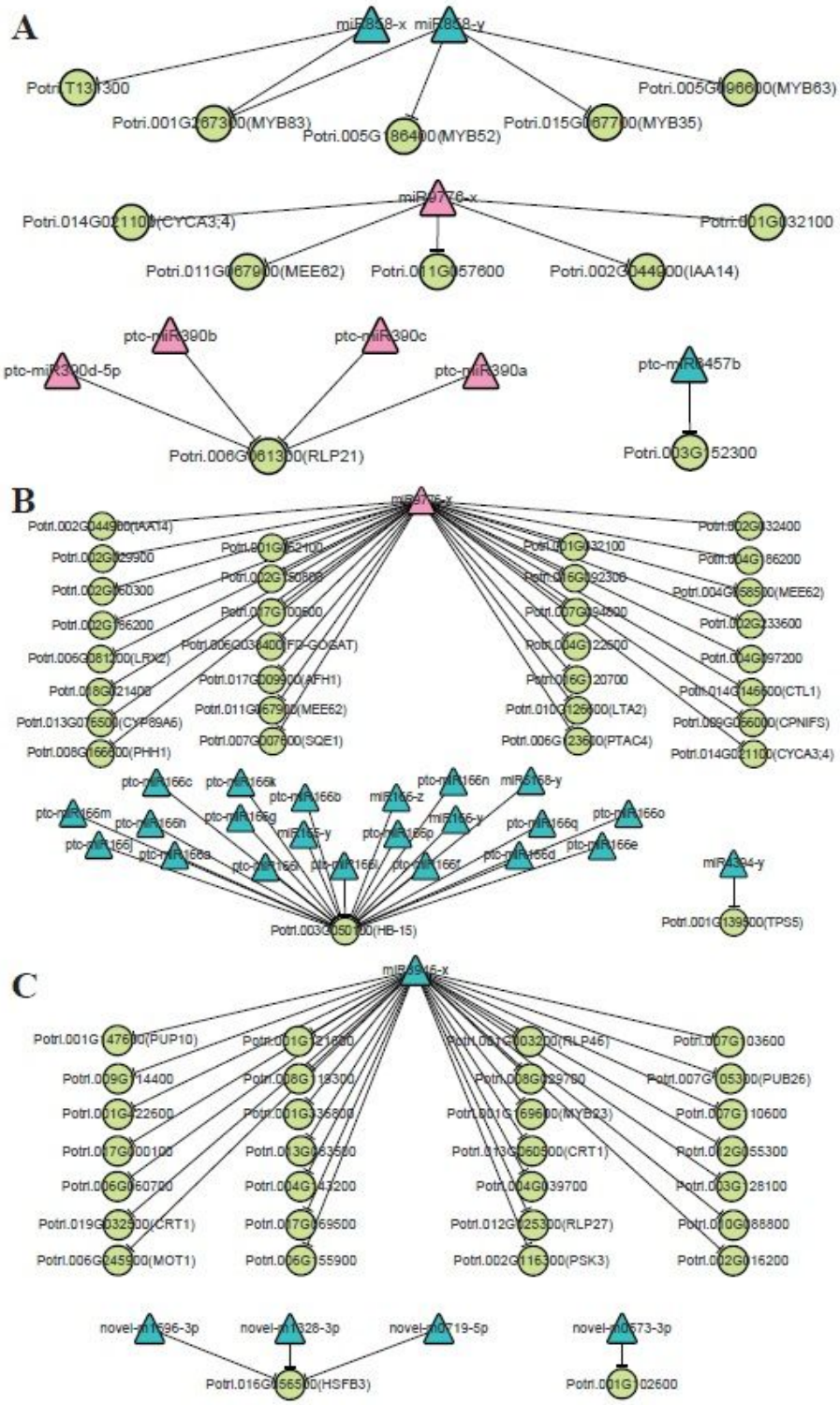

Figure 4

The regulatory relationships of DE-miRNAs and CTGs. (A) The regulatory relationships of DE-miRNAs and CTGs in PS vs TS. (B) The regulatory relationships of DE-miRNAs and CTGs in PS vs SS. (C) The regulatory relationships of DE-miRNAs and CTGs in TS vs SS. Pink represents up-regulated miRNA, Blue represents down-regulated miRNA, Green represents CTGs.

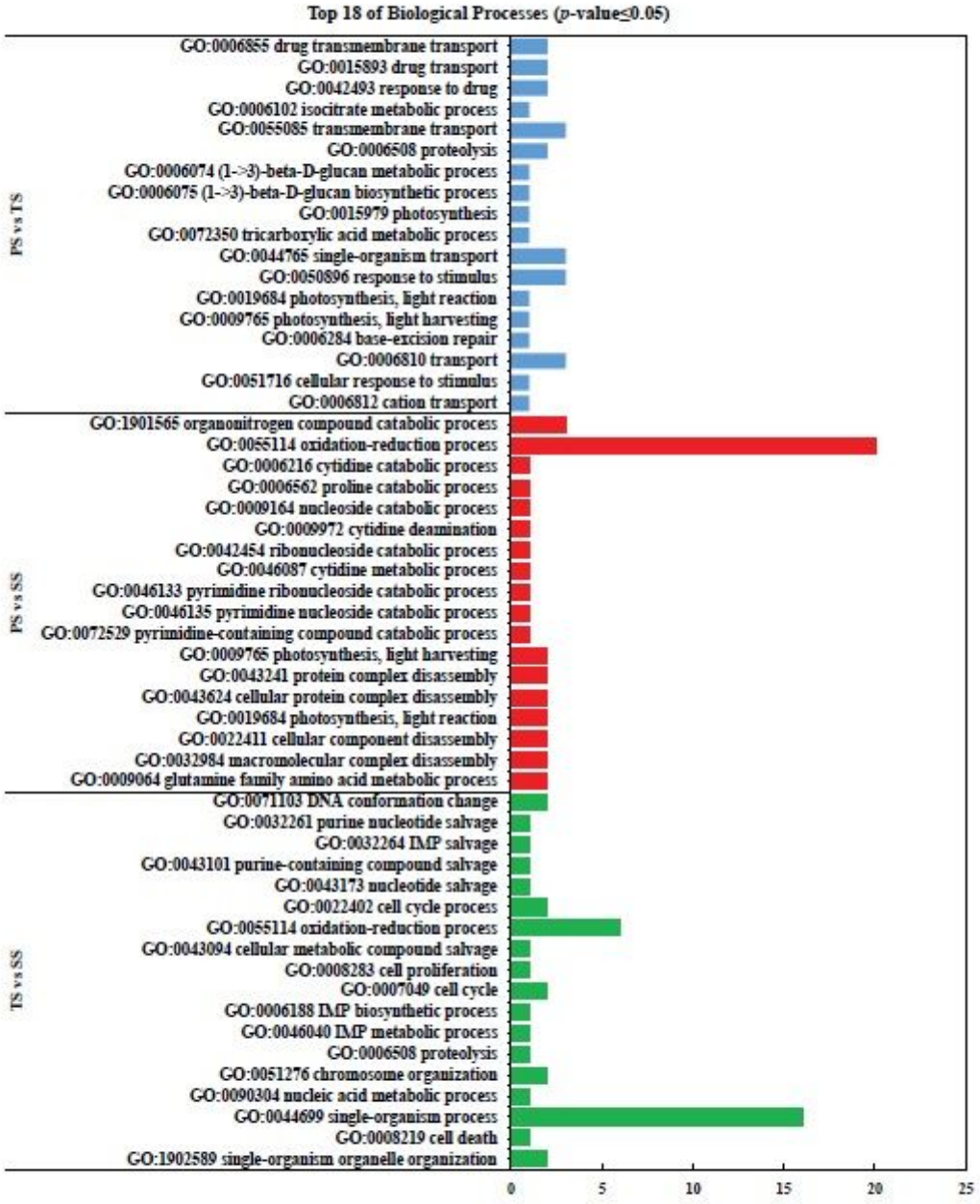

Figure 5

Heatmap of DE-miRNAs and TFs in CTGs with inverse relationships in their expression profiles from primary stem (PS) to transition stem (TS) and then to secondary stem (SS).

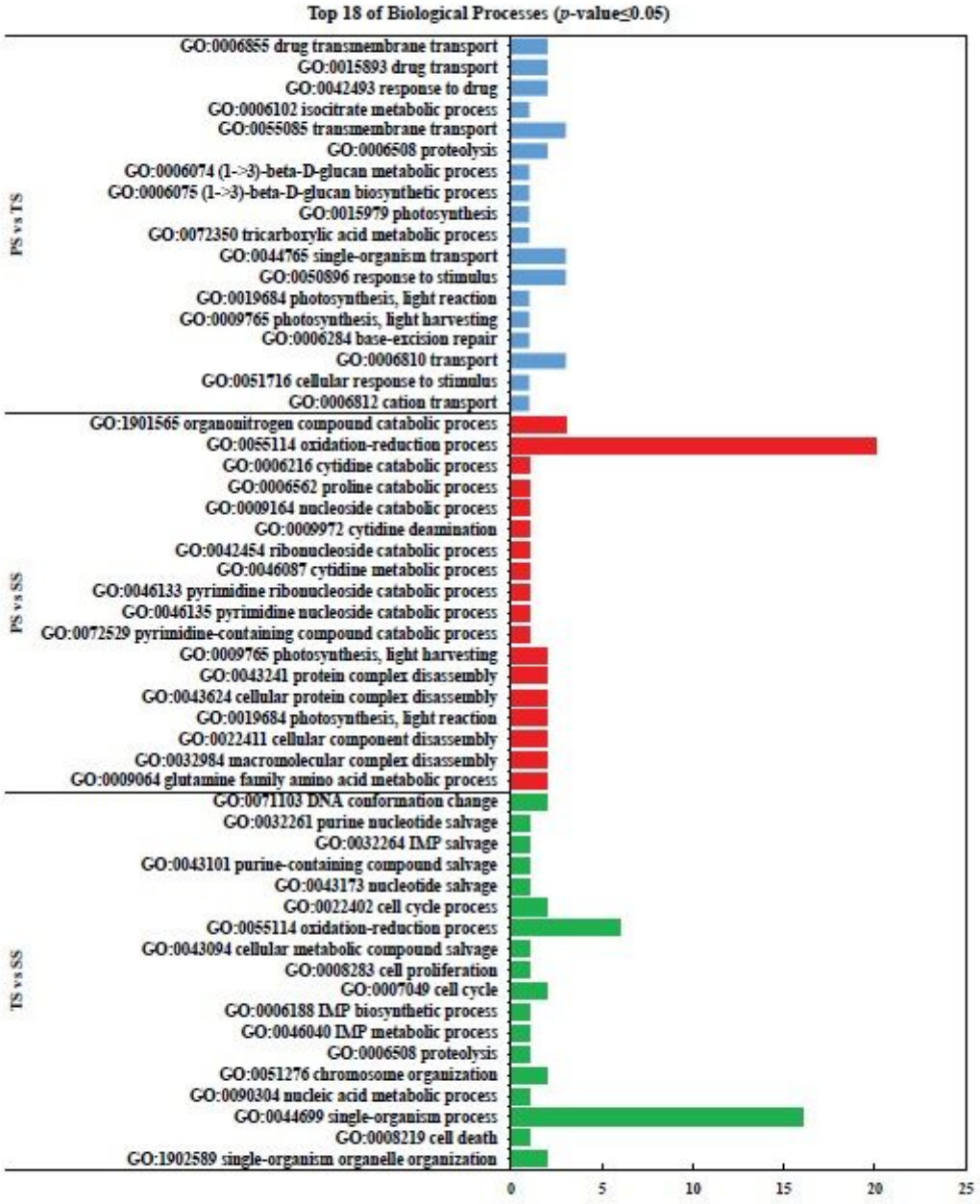

Figure 5

Heatmap of DE-miRNAs and TFs in CTGs with inverse relationships in their expression profiles from primary stem (PS) to transition stem (TS) and then to secondary stem (SS).

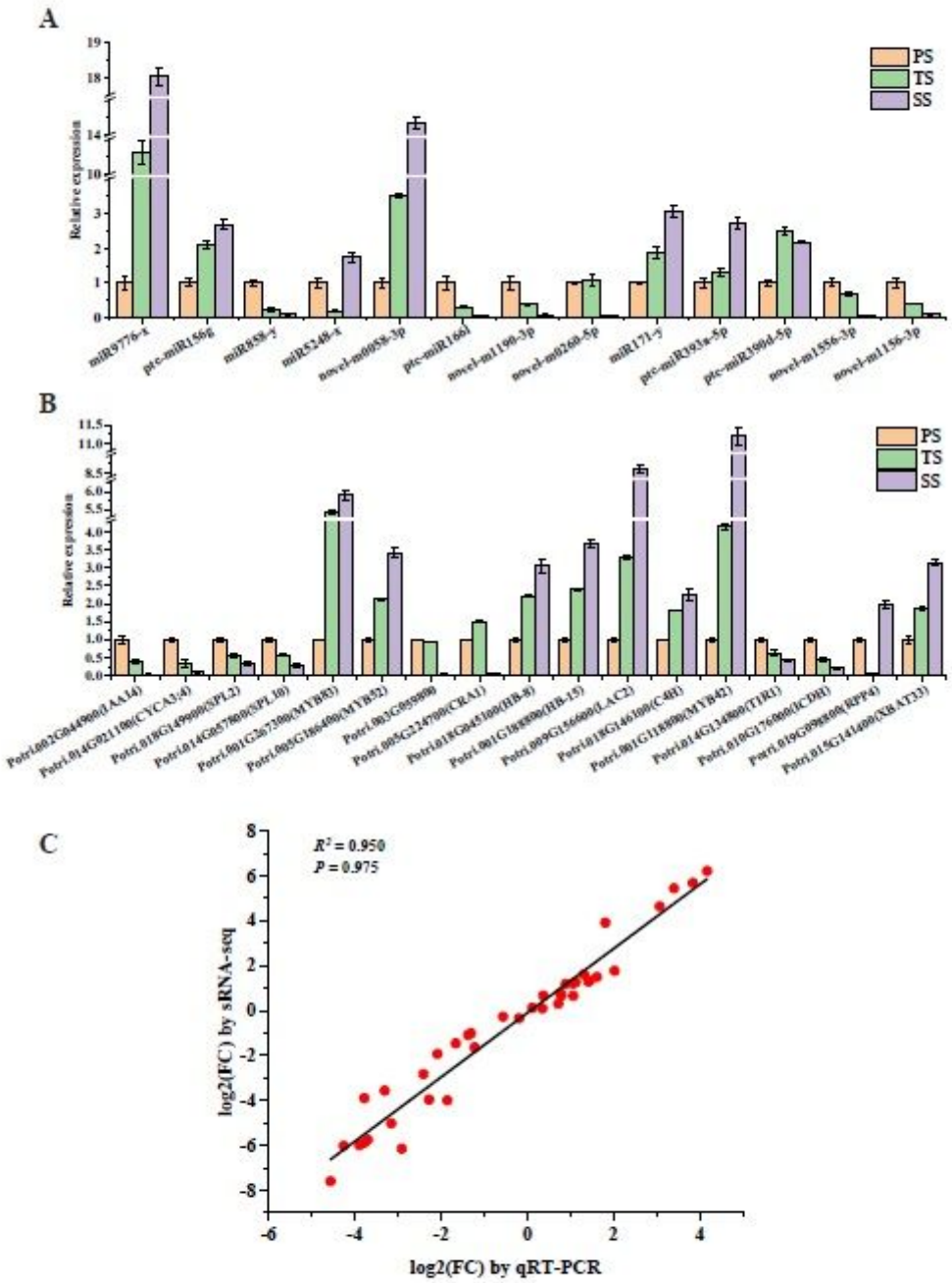

Figure 6

Expression profiles of miRNAs and CTGs which were structural mRNA-encoding genes related to wood formation of primary stem (PS) to transition stem (TS) and then to secondary stem (SS).

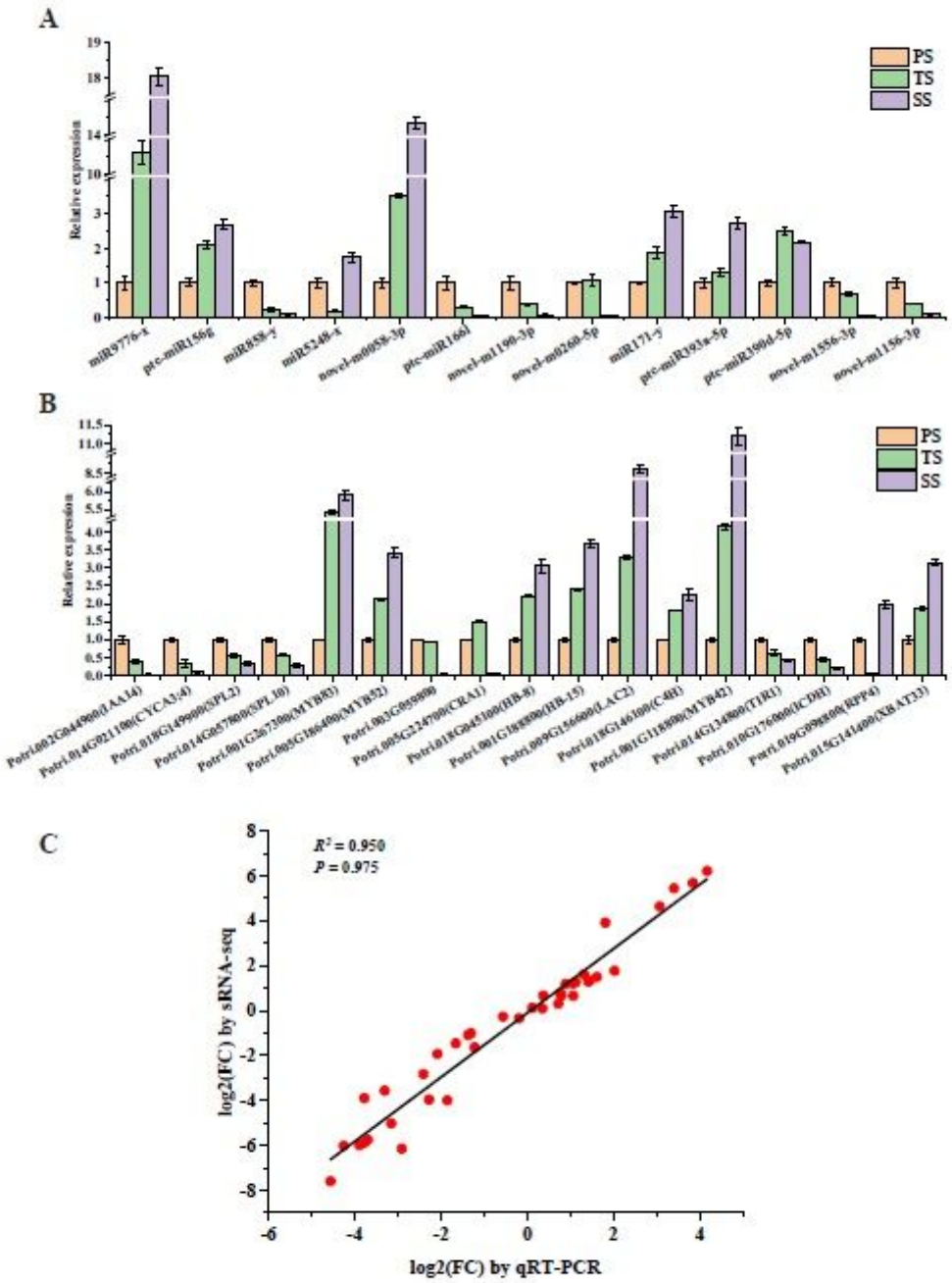

Figure 6

Expression profiles of miRNAs and CTGs which were structural mRNA-encoding genes related to wood formation of primary stem (PS) to transition stem (TS) and then to secondary stem (SS).

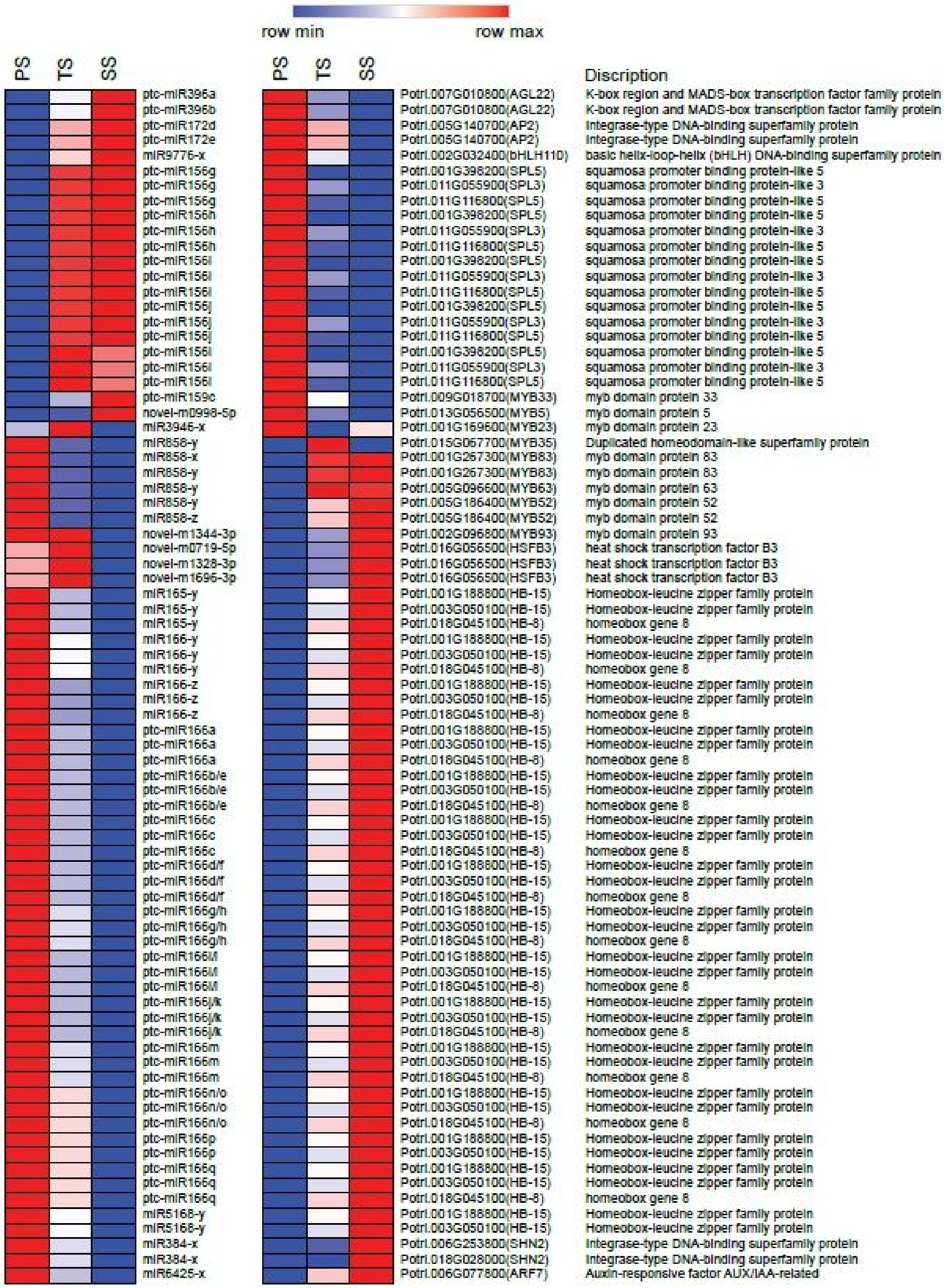

Figure 7

Top 18 of significant enriched biological processes represented by gene ontologies in the CTGs of DE-miRNAs. Blue represents significant enriched biological process for targets of DE-miRNA in PS vs TS. Red represents significant enriched biological process for targets of DE-miRNA in PS vs SS. Green represents significant enriched biological process for targets of DE-miRNA in TS vs SS. The x axis represents the number of genes. Corrected p-value ≤ 0.05 indicate significant enrichment.

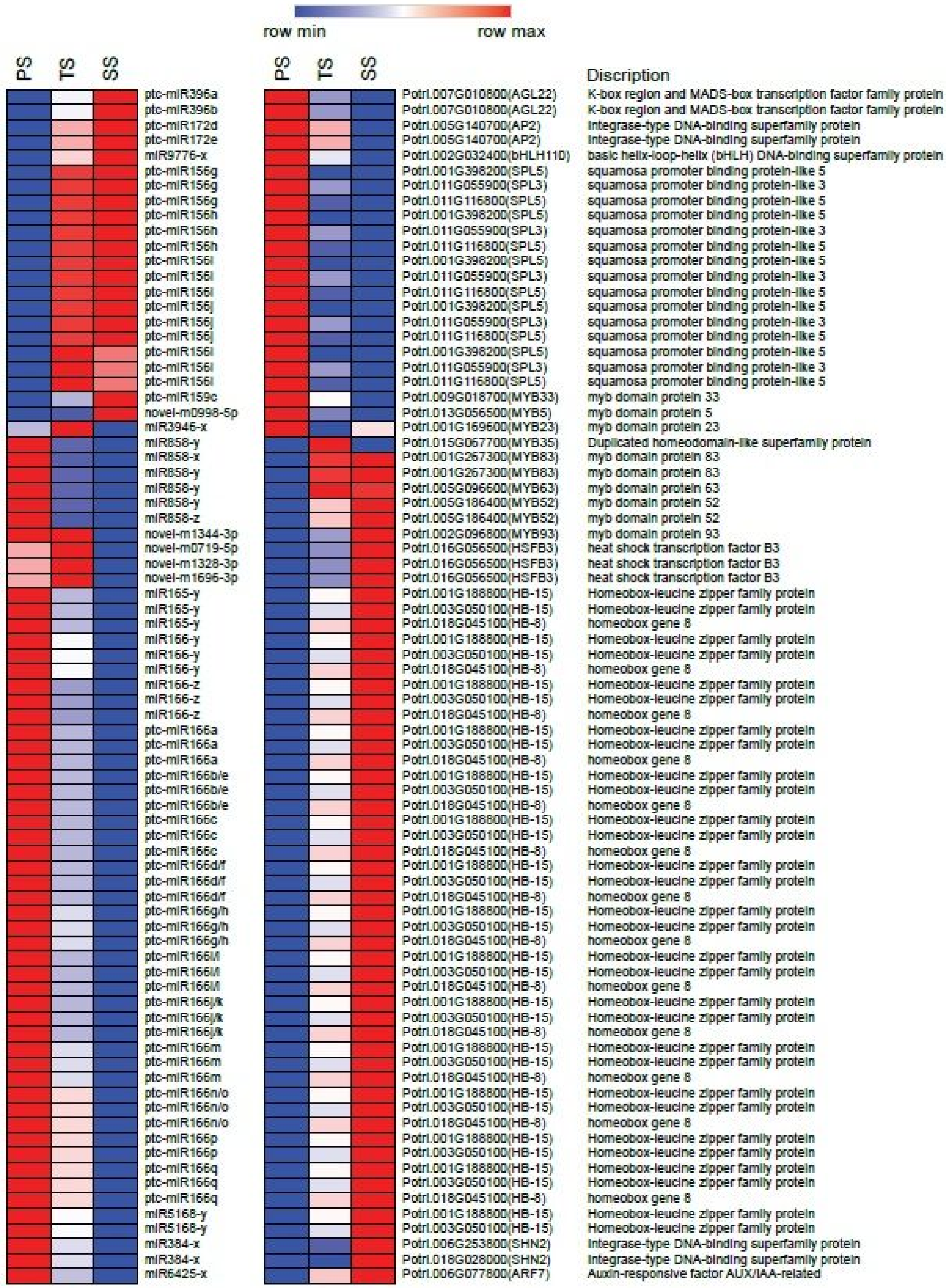

Figure 7

Top 18 of significant enriched biological processes represented by gene ontologies in the CTGs of DE-miRNAs. Blue represents significant enriched biological process for targets of DE-miRNA in PS vs TS. Red represents significant enriched biological process for targets of DE-miRNA in PS vs SS. Green represents significant enriched biological process for targets of DE-miRNA in TS vs SS. The x axis represents the number of genes. Corrected p-value ≤ 0.05 indicate significant enrichment.

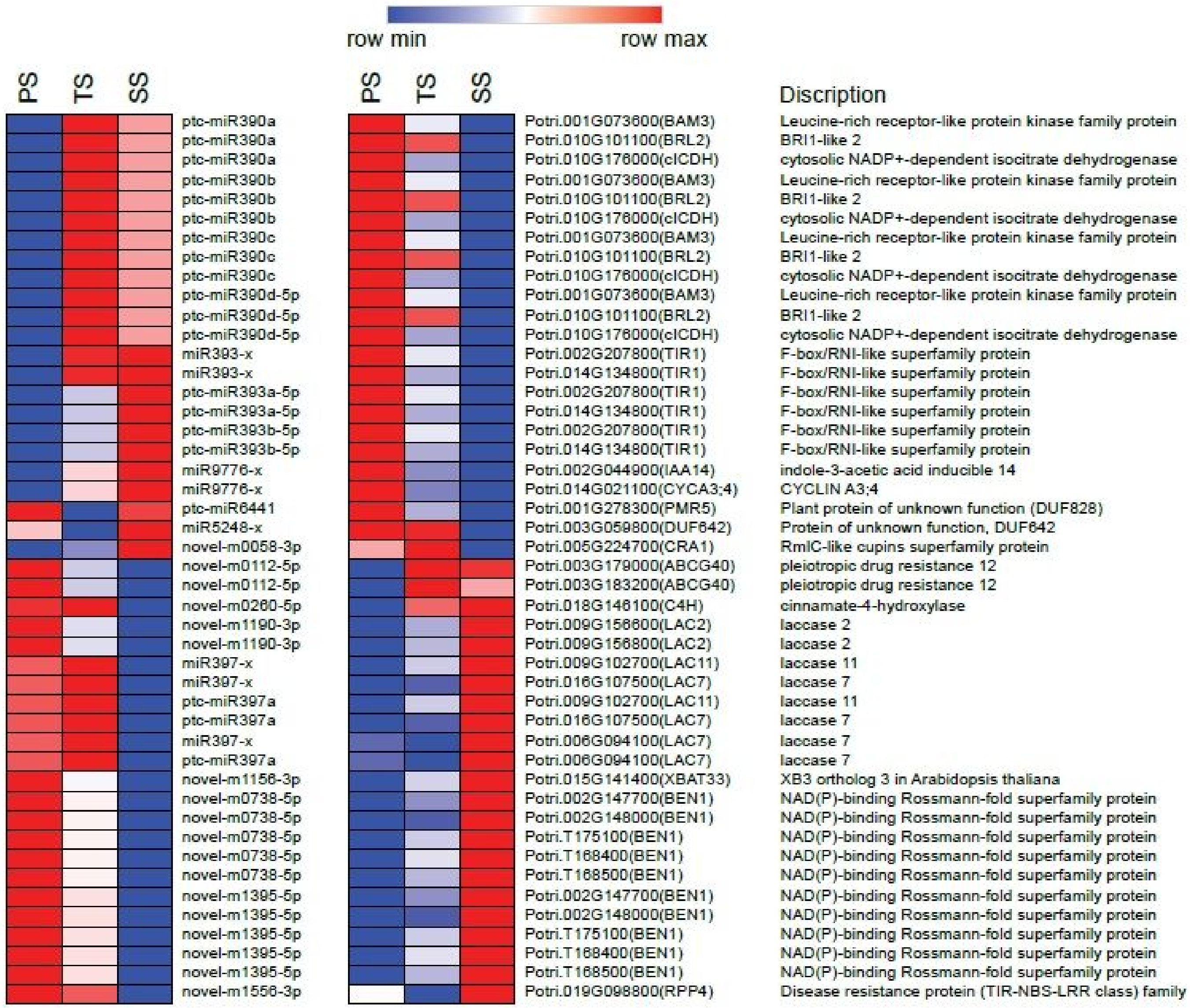

Figure 8

The expression levels of some representative miRNAs and CTGs. (A) the relative expression level distribution of 13 selected miRNAs (8 known miRNA and 5 novel miRNA) determined by RT-PCR in primary stem (PS), transition stem (TS) and secondary stem (SS). (B) the relative expression level distribution for the 17 genes targeted by 11 miRNAs. The expression levels of miRNAs and their mRNA targets were normalized to the level of 5.8S rRNA and β-actin, respectively. Each value is represented by mean ± SD of the triplicates of three biological replicates. (C) Linear regression analysis for comparing the results of RT-qPCR and small RNA-seq. The y axis represents the fold-change values by small RNA-seq, and the x axis represents the fold-change values by qRT-PCR. The R2 is 0.950 and correlation coefficient equals to 0.975. Solid lines represent linear regression lines.

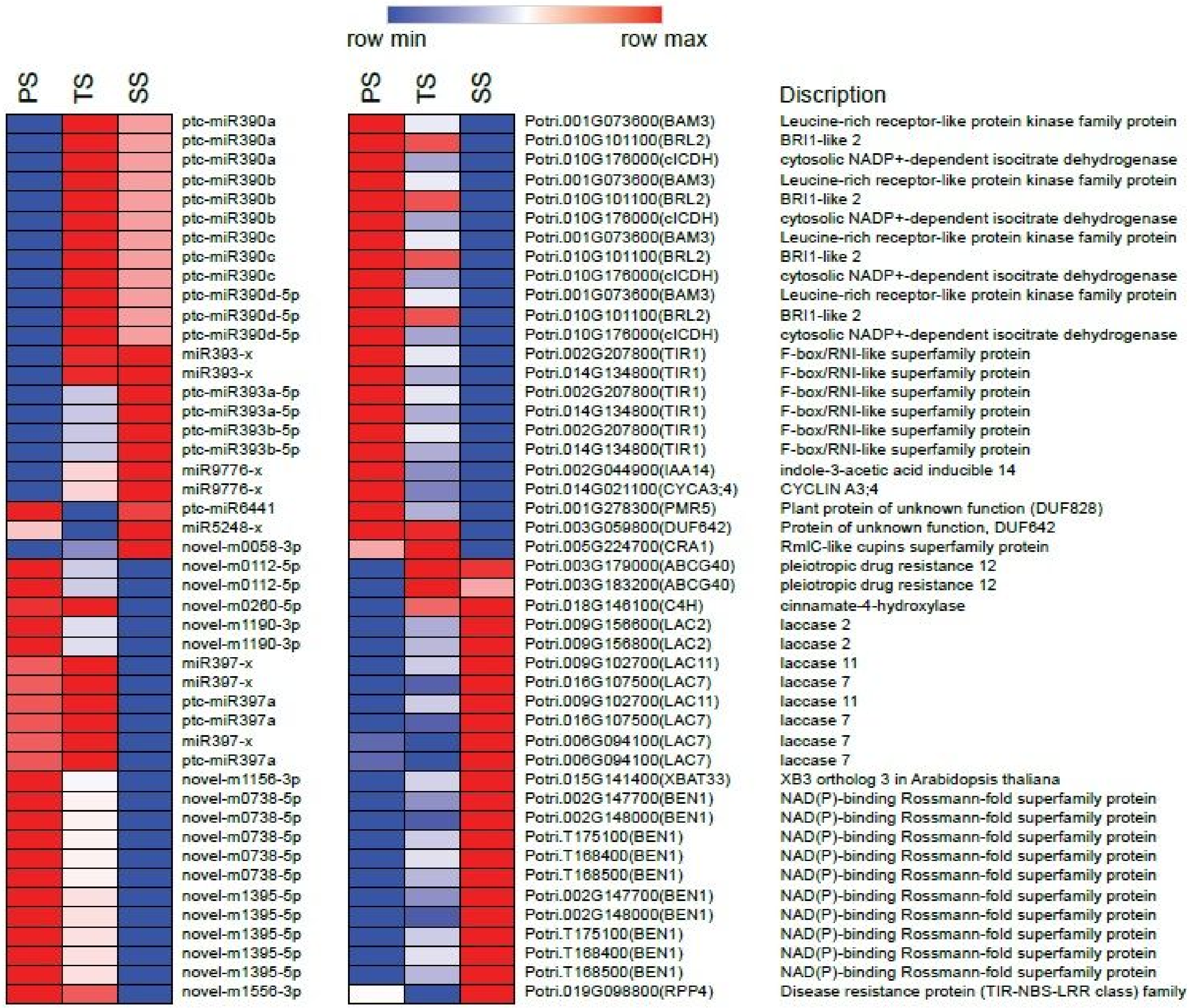

Figure 8

The expression levels of some representative miRNAs and CTGs. (A) the relative expression level distribution of 13 selected miRNAs (8 known miRNA and 5 novel miRNA) determined by RT-PCR in primary stem (PS), transition stem (TS) and secondary stem (SS). (B) the relative expression level distribution for the 17 genes targeted by 11 miRNAs. The expression levels of miRNAs and their mRNA targets were normalized to the level of 5.8S rRNA and β-actin, respectively. Each value is represented by mean ± SD of the triplicates of three biological replicates. (C) Linear regression analysis for comparing the results of RT-qPCR and small RNA-seq. The y axis represents the fold-change values by small RNA-seq, and the x axis represents the fold-change values by qRT-PCR. The R2 is 0.950 and correlation coefficient equals to 0.975. Solid lines represent linear regression lines.

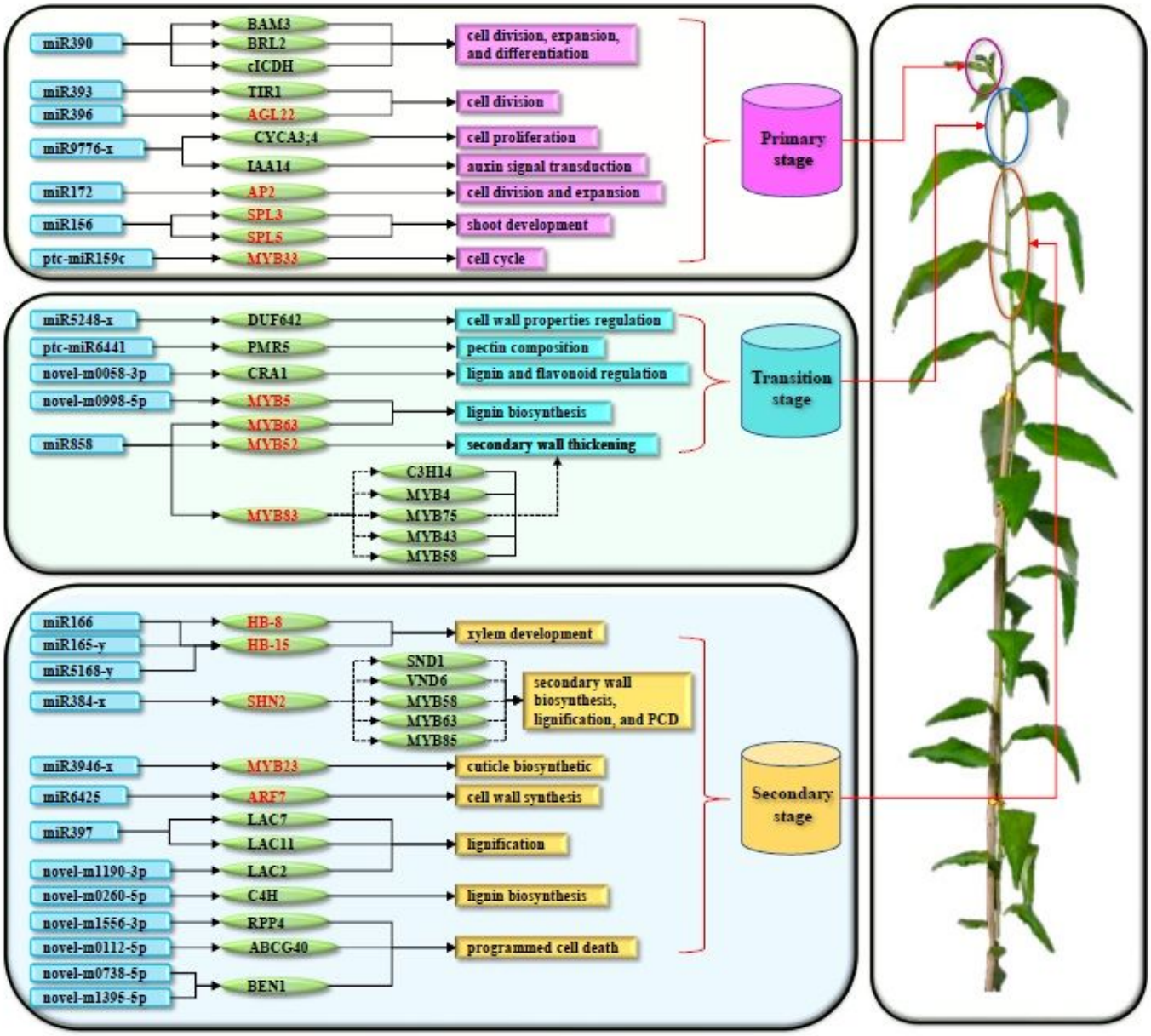

Figure 9

The identified miRNAs and target genes that were associated wood formation. Each blue arc edge rectangle represents a miRNA; each green ellipse contains a target gene (Red font means TF identified in this study); each rectangle shows the function of a target gene. The solid line represents the relationship identified in this study while the dotted line represents the relationship identified in previous studies.

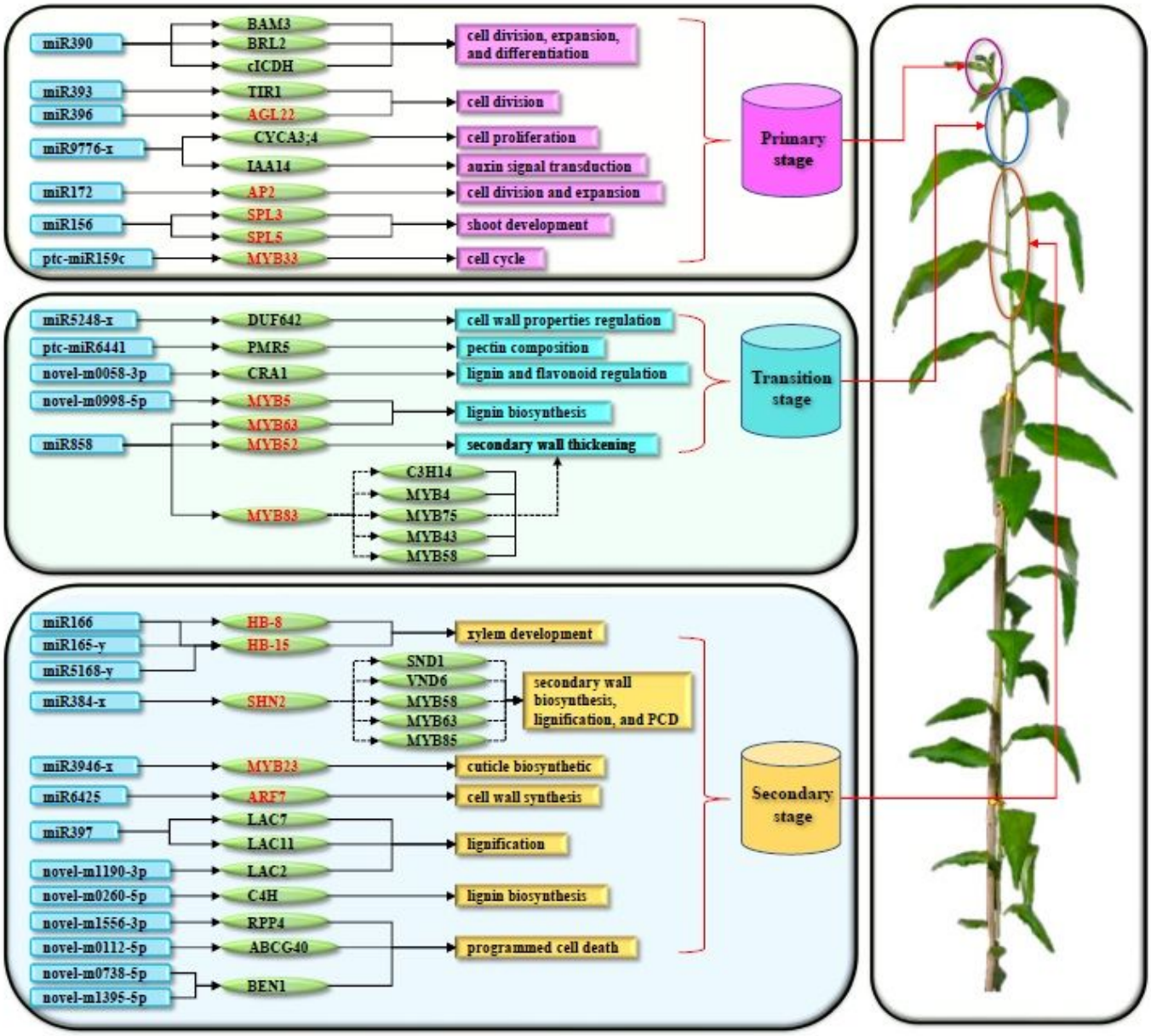

Figure 9

The identified miRNAs and target genes that were associated wood formation. Each blue arc edge rectangle represents a miRNA; each green ellipse contains a target gene (Red font means TF identified in this study); each rectangle shows the function of a target gene. The solid line represents the relationship identified in this study while the dotted line represents the relationship identified in previous studies.

Supplementary Files

This is a list of supplementary files associated with this preprint. Click to download.

- SupplementalFigure12.docx
- SupplementalFigure12.docx

- SupplementalTableS1.docx
- SupplementalTableS1.docx
- SupplementalTableS1012.xlsx
- SupplementalTableS1012.xlsx
- SupplementalTableS1315.xlsx
- SupplementalTableS1315.xlsx
- SupplementalTableS1618.xlsx
- SupplementalTableS1618.xlsx
- SupplementalTableS1921.xlsx
- SupplementalTableS1921.xlsx
- SupplementalTableS2.xlsx
- SupplementalTableS2.xlsx
- SupplementalTableS2224.xlsx
- SupplementalTableS2224.xlsx
- SupplementalTableS25.xlsx
- SupplementalTableS25.xlsx
- SupplementalTableS26.xlsx
- SupplementalTableS26.xlsx
- SupplementalTableS3.xlsx
- SupplementalTableS3.xlsx
- SupplementalTableS46.xlsx
- SupplementalTableS46.xlsx
- SupplementalTableS79.xlsx
- SupplementalTableS79.xlsx